Available online at www.sciencedirect.com
SCIENCE DIRECT
Organic Geochemistry 37 (2006) 72–97
Organic Geochemistry
www.elsevier.com/locate/orggeochem

Comparative molecular biomarker assessment of phytoplankton paleoproductivity for the last 160 kyr off Cap Blanc, NW Africa

Meixun Zhao [a,*], Jennifer L. Mercer [b,1], Geoffrey Eglinton [c], Matthew J. Higginson [d], Chi-Yue Huang [e]

[a] School of Chemistry and Chemical Engineering, Ocean University of China, Qingdao 266003, PR China
[b] Department of Earth Sciences, Dartmouth College, Hanover, NH 03755, United States
[c] Department of Marine Chemistry and Geochemistry, Woods Hole Oceanographic Institution, Woods Hole, MA 02543, United States
[d] Forensic Alliance Limited, F5 Culham Science Centre, Abingdon, Oxfordshire OX14 3ED, UK
[e] Department of Earth Sciences, National Cheng Kung University, Tainan, Taiwan

Received 10 January 2005; accepted 10 August 2005
(returned to author for revision 9 April 2005)
Available online 2 November 2005

Abstract

We report high resolution molecular abundance data for alkenones, dinosterol, long chain diols and *n*-alkanols from ODP Site 658 (20°45′N, 18°35′W; 2263 m water depth). These data are compared with previously reported data for TOC, chlorins, opal and long chain *n*-alkanes. The contents and mass accumulation rates (MARs) of chlorins are used as total phytoplankton productivity proxies, while the contents and MARs of opal, dinosterol, alkenones and diols are used as productivity proxies for diatoms, dinoflagellates, haptophytes and eustigmatophytes/diatoms, respectively. Five high productivity intervals (HPIs) are identified: two at the glacial/interglacial transition boundaries of 132–122 and 15–8 ka, two within the warmer periods of MIS 3 (50–30 ka) and the late Holocene (4–0 ka), and one within the glacial period of MIS 4 (67–60 ka). Productivity was lowest during both the penultimate glacial maximum of MIS 6 (150–140 ka) and the last glacial maximum (22–18 ka), as revealed by both the total phytoplankton and individual phytoplankton productivity indicators. Phytoplankton community structure changed significantly over the last 160 kyr. The Termination I&II HPIs were characterized by higher opal content, possibly reflecting increased diatom contributions to total productivity. Eustigmatophyte/diatom and haptophyte contributions were higher during MIS 5, but decreased toward the Holocene. Dinosterol revealed an opposite trend, with the highest contribution in the Holocene. We ascribe such changes in phytoplankton communities to the effects brought about by the varying amounts and nature of nutrient inputs contributed regionally by eolian dusts, river influxes, ocean currents and upwelling water masses.

1. Introduction

Increasing concern over the global climatic effects of rising atmospheric CO_2 concentrations from fossil fuel burning has prompted reconstructions of the record of natural CO_2 variability.

* Corresponding author.
E-mail addresses: Meixun.Zhao@Dartmouth.Edu, maxzhao04@yahoo.com (M. Zhao).
[1] Now at: Department of Atmospheric Science, The University of Wyoming, Laramie, WY82072.

0146-6380/$ - see front matter © 2005 Elsevier Ltd. All rights reserved.
doi:10.1016/j.orggeochem.2005.08.022

Several records obtained using ice cores (Barnola et al., 1987; Petit et al., 1999) and deep sea sediments (Shackleton et al., 1983; Jasper and Hayes, 1990) have shown that past atmospheric CO_2 concentration has varied by 40% between glacial and interglacial periods. Since the oceans contain 60 times more carbon than the atmosphere (Broecker and Peng, 1982), it has been proposed that CO_2 exchanges between the atmosphere and the oceans were largely responsible for past pCO_2 oscillations (Broecker and Peng, 1989). Transport of carbon from the surface ocean to the deep sea and ultimate sediment burial is to a large extent controlled by the "biological pump" (Berger et al., 1989), although other physical processes are also very important (Berger and Keir, 1984; Boyle, 1988; Broecker and Peng, 1989). Thus, the accurate reconstruction of paleoproductivity is critical for understanding the carbon cycle in the past and for predicting the fate of anthropogenic carbon in the future. Several approaches have been advanced for quantitative estimation of paleoproductivity, such as those based on the sedimentary contents of total organic carbon (TOC), siliceous fossils, foraminiferal species and barite (Pokras, 1987; Mix, 1989; Sarnthein et al., 1992; Paytan et al., 1996; Abrantes, 2000; Anderson et al., 2002). In this paper, we apply this general approach, but using mainly biomarker proxies, to a deep sea sediment site, ODP Site 658 (Fig. 1), cored on the continental slope west of Cap Blanc (20°45′N, 18°35′W) in 2263 m water depth.

1.1. Biomarkers and phytoplankton productivity

Biomarkers in marine sediments have been used as proxies for total and specific phytoplankton group paleoproductivity. For example, chlorin accumulation rate has been used as a molecular indicator of total phytoplankton paleoproductivity (Harris et al., 1996). This approach is based on the fact that chlorophyll *a*, one of the pigments required for photosynthesis, is present in all aerobic photosynthetic organisms and is the most abundant chlorophyll in the biosphere (Welschmeyer and Lorenzen, 1985). Its concentration in the photic zone has been used as a means of estimating algal biomass and productivity (Longhurst et al., 1995). However, following senescence, water column transformation and early sedimentary diagenesis, less than 1% of the chlorophyll production is typically preserved in marine sediments as chlorins (Keely et al., 1990; Eckardt et al., 1992; Shankle et al., 2002). Hence, chlorins were early considered to be

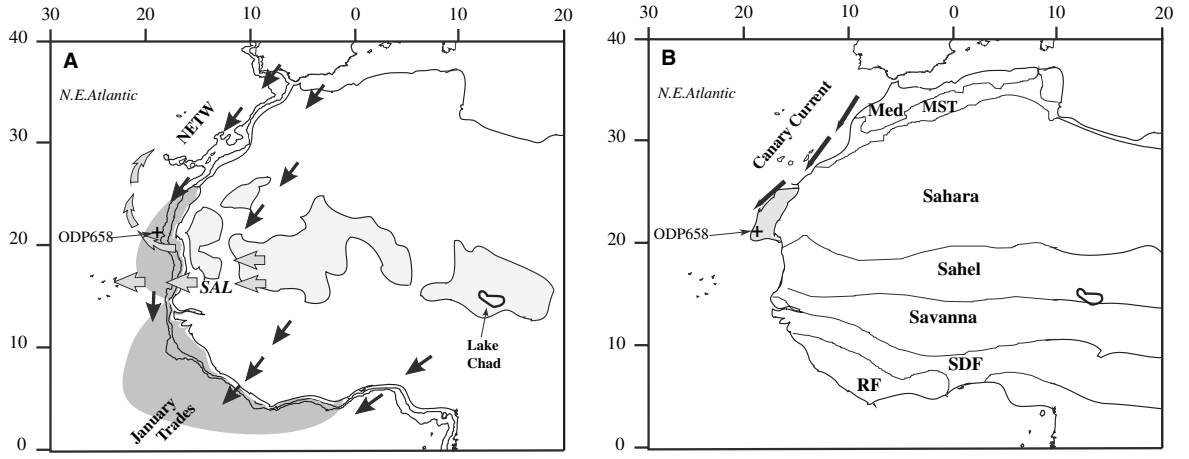

Fig. 1. (A) Present day major wind belts, dust source and deposition regions of northwest Africa and the northeast Atlantic. SAL = Saharan Air Layer; NETW = North East Trade Wind. The darker shaded areas over the Northeast Atlantic Ocean are those for which high occurrences of atmospheric haze are recorded; northern zone during summer and southern zone during winter. Bathymetry: 200 and 2000 m. The plus symbol (+) denotes the location of ODP Site 658. The lighter shaded areas over the continent are major dust source areas delineated by Goudie and Middleton (2001) based on the high values (>15) of annual mean Aerosol Index for the Sahara. (B) Present day surface ocean currents (Canary Current, solid arrow) and upwelling regime (shaded area) of the northeast Atlantic and vegetation zones of northwest Africa (White, 1983). From North to South: Med, Mediterranean vegetation zone; MST, Mediterranean-Saharan transitional steppes; Sahara, absolute desert, desert and semi-desert; Sahel, semi-desert grassland to *Acacia* wooded grassland; Savanna, dry savannas and woodland; SDF, semi-deciduous forest; RF, tropical rain forest.

of little use as a quantitative estimate of paleoproductivity (Eppley and Peterson, 1979; Repeta et al., 1992). Furthermore, the uncertainty remains as to what extent chlorin concentration, or MAR variation in marine sediment is a result of changes in surface productivity or of sedimentary preservation (Furlong and Carpenter, 1988; Calvert and Pedersen, 1992). Despite these uncertainties, Harris et al. (1996) demonstrated the potential of chlorins as a proxy of Quaternary marine productivity by correlating chlorin MAR maxima with peaks of other productivity indicators, such as biogenic opal MAR and TOC MAR over the last 350 kyr from ODP Site 658. Thus, chlorins have been applied for reconstructing paleoproductivity in the South (Summerhayes et al., 1995) and North Atlantic (Higginson, 2000), in the Northeastern (Schubert et al., 1998) and Northwestern Arabian Sea (Altabet et al., 2002; Higginson et al., 2004), and in the South China Sea (Higginson, 2000; Higginson et al., 2003). Similarly, loliolide and isololiolide, the degradation products of carotenoid pigments, have been used to estimate marine productivity (Hinrichs et al., 1999; Versteegh and Zonneveld, 2002). Steryl chlorin esters (SCEs) have also been shown to have potential for phytoplankton community assessment (Dahl et al., 2004).

Alkenones are probably the most thoroughly studied lipid biomarkers of marine origin, due to the increasing use of the $U^{K'}_{37}$ index to reconstruct past sea surface temperature (SST; Brassell et al., 1986; Prahl and Wakeham, 1987; Eglinton et al., 2001). Their biological source is restricted to a narrow range of marine algae belonging to the haptophyta, of which *Emiliania huxleyi* is the most important contemporary oceanic member (Volkman et al., 1980a,b; Marlowe et al., 1990). Their abundances and accumulation rates have been used to estimate haptophyte productivity and total marine productivity (Prahl et al., 1993; Rostek et al., 1997; Villanueva et al., 1997, 1998; Henriksson et al., 2000; Werne et al., 2000; Pailler et al., 2002; Versteegh and Zonneveld, 2002; Calvo et al., 2004; Higginson and Altabet, 2004; Moreno et al., 2004; Seki et al., 2004).

The long chain C_{28}, C_{30} and C_{32} alkyl diols are often very abundant in marine sediments (Poynter et al., 1989a; Versteegh et al., 1997; Schouten et al., 2000; Versteegh et al., 2000; Méjanelle et al., 2003; Sinninghe Damsté et al., 2003). There are a number of positional isomers, but the C_{30} and C_{32}1, 15-diols are frequently dominant (Ferreira et al., 2001). Mediterranean sapropels have high concentrations of the C_{30}-1,15-diols, with minor amounts of the corresponding C_{32} isomer and only traces of the 1,14 diols. On the other hand, Versteegh et al. (2000), Méjanelle et al. (2003) and Sinninghe Damsté et al. (2003) found that the alkyl diols in the sediments below the upwelling zone off Walvis Bay are dominated by the C_{30}-1,14-diol. This compound was also the main diol beneath the Oman upwelling region (ten Haven et al., 1989). Sinninghe Damsté et al. (2003) concluded that the 1,14 alkyl diols are indicators of high nutrient conditions in the photic zone and suggested that the 1,13- and 1,15-diols are likely produced by marine yellow-green microalgae, such as the eustigmatophytes. Méjanelle et al. (2003) reported that the alkyl diols produced by the eustigmatophyte *Nannochloropsis* have the C_{32}-1,15-diol as the most abundant compound, accompanied by some C_{30}, C_{34} and C_{36}-1,15-diols and C_{30}-1,13-diols. On the other hand, the 1,14-diols are produced by diatoms such as the widespread genus *Proboscia*. It is probable that there are significant unidentified algal sources. In spite of these uncertainties, these alkyl diols have been used as biomarkers in paleoenvironmental reconstruction. For example, their abundance in marine sediments was used as one of the indicators of marine algal productivity off NW Africa at ODP Sites 658 and 660 (Poynter et al., 1989a) and in the SE Atlantic below the highly productive waters on the African continental margin (Hinrichs et al., 1999), where for two cores each spanning the last 76 kyr, the alkyl diols showed a close positive relationship with other productivity proxies, such as alkenones and dinosterol. These biomarkers generally have higher concentrations during the glacial periods, probably reflecting higher productivity. A diol index has been introduced by Versteegh et al. (1997) based on the relative abundances of the 1,15-$C_{30}(\omega 16)$ and the 1,15-$C_{32}(\omega 18)$ isomers. From limited data, this index has been proposed to reflect the surface hydrography where the compounds are synthesized.

Analyses for the alkyl diol isomers, e.g., 1,15-, 1,14-, etc. and homologues, e.g., C_{28}, C_{30}, etc., plus determination of the corresponding keto-ols and hydroxy alkenoates would provide an excellent data base for evaluation in conjunction with other parameters, such as upwelling and nutrient indicators. Work to date, notably the surveys made of South West Africa, e.g., the Congo vs Walvis Bay,

indicates that the diols are sensitive indicators of hydrographic conditions in the photic zone, reflecting mainly nutrient levels.

Dinosterol is the major sterol in many species of dinoflagellates (Boon et al., 1979; Volkman et al., 1998), although it also has been reported in a few diatoms (Volkman et al., 1998). Its occurrence and that of its saturated hydrocarbon counterpart in sediments (Moldowan et al., 1996) have been used as indicators of dinoflagellate contribution to sedimentary organic matter, while the stratigraphic changes in dinosterol content have also been used to infer changes in marine productivity and dinoflagellate productivity. Increases of dinosterol content in recent (20th century) sediment samples from the Santa Barbara Basin and the Chesapeake Bay correlate well with regional dinoflagellate bloom events (Kennedy and Brassell, 1992; Zimmerman and Canuel, 2002). On a glacial/interglacial timescale, dinosterol content changes indicate that dinoflagellate surface productivity was higher during the glacial periods in the Southern Ocean (Ikehara et al., 2000) and the Atlantic (Henriksson et al., 2000), but in contrast, higher during the interglacial stages and deglacials along the California continental margin (Mangelsdorf et al., 2000) and in the Japan Sea (Ishiwatari et al., 1999).

1.2. Biomarkers and phytoplankton community structure

For today's environment, changes in competition and consequently phytoplankton community structure due to differing biological responses to varying nutrient concentrations and other environmental factors can be clearly demonstrated by direct cell counting and DNA, pigment and lipid biomarker analyses (Abrantes et al., 2002; Wakeham et al., 2002) and by models (Smayda and Reynolds, 2001). Detailed pigment data offer a useful tool for the study of phytoplankton community structure in present day oceanic environments (Mackey et al., 1996; Mackey et al., 2002; Qian et al., 2003). Qian et al. (2003) studied the spatial and temporal variability of phytoplankton biomass in the waters of the Gulf of Mexico using pigment analysis and classified the main classes as haptophytes, prokaryotes (cyanobacteria, prochlorophytes), diatoms and dinoflagellates. However, many pigment compounds experience diagenesis and lose their structural information relatively quickly in the sediments. Hence, one can not readily use this approach to reconstruct paleocommunity structures from the sedimentary record. The non-pigment lipid biomarkers, although less specific, offer another method for paleoreconstruction. Wakeham et al. (2002) carried out detailed lipid biomarker analyses of trap materials collected in the Arabian Sea off Oman. They assessed the contribution of each biomarker and hence source organism, by normalizing biomarker fluxes to the total organic carbon fluxes and proposed that the progression in biomarker flux peaks through time should correspond to a succession in the source organisms that produced them. They concluded that biomarker fluxes fluctuate in time and space as a reflection of biological production and of community structure and succession, as controlled by variations in hydrography and nutrient regimes.

Schubert et al. (1998) were among the first to use the multi-biomarker-based approach to assess the paleophytoplankton community structure at a site (94KL) in a monsoon-driven upwelling area in the northern Arabian Sea, employing chlorins for total phytoplankton, brassicasterol for diatoms, alkenones for haptophytes and dinosterol for dinoflagellates. Concordant concentration maxima for these proxies and TOC over the last 200,000 yr were used to infer that the relative contributions of the phytoplankton groups were roughly uniform at the millennial timescale, with major contributors being diatoms, dinoflagellates and haptophytes. They argued that, with the core location located beneath the oxygen minimum zone (OMZ), the contents of these biomarkers would not be significantly affected by preservation artifacts. However, they also noticed that double peaks in TOC and chlorins at ca. 135 kyr could be resolved into a high dinosterol contribution (first peak) and high alkenone and brassicasterol contributions (second peak). They pointed to the considerable potential of the multiple biomarker method, as it is able to distinguish between different contributors. Other studies have provided a plethora of evidence that community structure has changed on glacial–interglacial timescales in response to changes in climate and in nutrient inputs. Seki et al. (2004) reconstructed changes in community structure for the Sea of Okhotsk over the last 30 kyr using the mass accumulation rates of alkenones, $CaCO_3$, and biogenic opal. They concluded that the shift in the dominant phytoplankton species from coccolithophorid (*E. huxleyi*) during deglaciation to diatoms in the late Holocene was probably caused by an increase in silicate supply

to the euphotic layer. Dahl et al. (2004) used SCEs to estimate the phytoplankton community change in the Cariaco Basin during the Younger Dryas (YD) cold event. They observed an increase in the diatom population but a decrease in the dinoflagellate population, in response to enhanced upwelling. Using sterol and alkenone biomarkers, Werne et al. (2000) also observed a diatom-dominated phytoplankton community in the Cariaco Basin during the YD which became coccolithophore-dominated during the Holocene. Schulte and Bard (2003) reported the abundances of alkenones, sterols, diols and ketols for a site on the Maldives platform of the Indian Ocean. They argued that the biomarker abundances could serve as qualitative proxies for changes in paleoproductivity and used the lipid/TOC records to reconstruct the productivity of the planktonic community over the last 320 kyr. Their finding was that the community did not change significantly during this time. Menzel et al. (2003) used the biomarker approach as being "representative of four major classes of marine primary producers – haptophytes (alkenones), diatoms (loliolides, etc.), dinoflagellates (dinosterol) and eustigmatophytes (alkyl diols and ketols). Their results from sites in a transect in the Mediterranean through Pliocene sapropel horizons, suggested that the phytoplankton composition was not influenced by SST but rather was controlled by the nutrient supply. Similarly, the parallelism between *n*-alkane and brassicasterol fluxes in the Tasman Sea area was taken to indicate that diatom productivity responded to increased dust input during the glacials (Calvo et al., 2004).

1.3. Terrigenous input and ocean productivity

Both rivers and eolian dust contribute terrigenous components to marine sediments. River input is generally higher during the warmer and more humid interglacial periods (Tiedemann, 1991; Bertrand et al., 1996). Dust supply can be influenced by several processes. The first is the extent of lift off from the continent. Rapid changes can occur in the availability and characteristics of the dust sources consequent upon climatic and vegetation changes. Thus, both the chemistry and mineralogy of the dust are variable. Lake Chad and associated areas (Fig. 1), rich in playas and paleolake deposits, are major sources of dust (Eglinton et al., 2002; Prospero et al., 2002), especially in the past. The transcontinental Sahel zone running West to East to the South of the Sahara is subject to seasonal loss of grass cover due to fire and to desiccation of ephemeral river and lacustrine areas, exposing fine soils and alluvial sediments to wind erosion; the Central Mountain Massif (Tibesti mountains), constantly eroded by sand storms, is extremely rich in iron (Goudie and Middleton, 2001) and to the north, the Atlas mountain regions have carbonate rocks with different element contents (Fig. 2.1). Dust delivered to the Atlantic (Fig. 2.4) depends on many factors, notably climate strength and direction of wind systems, hydrographic regime and the consequential vegetation cover.

Saharan dusts contain high amounts of iron and silica (Goudie and Middleton, 2001; Eglinton et al., 2002; Perez-Marrero et al., 2002), as well as other minerals and elements, which would stimulate phytoplankton growth. The immediate fertilizing effect of dust on productivity of open ocean waters has been well established (Martin and Fitzwater, 1988; Price and Morel, 1990; Boyd et al., 2000; Bowie et al., 2001; Chrisholm et al., 2001; Bishop et al., 2002; Mills et al., 2004). The SOIREE experiment (Bowie et al., 2001) with added iron showed that large pennate diatoms and autotrophic flagellates (mainly haptophytes) responded quickly to iron input. The bloom can last up to 2 yr due to biogeochemical cycling in the surface waters. Hence, intermittent major dust storms even on a yearly basis would be expected to result in apparently continuous blooms on a geological timescale. Mills et al. (2004) conducted iron fertilization experiments in the eastern tropical North Atlantic, a region rich in diazotrophs and strongly impacted by Saharan dust input. They showed that the region's primary productivity was nitrogen-limited and that nitrogen fixation was co-limited by iron and phosphorus. Saharan dust addition evidently stimulated nitrogen fixation, by supplying both iron and phosphorus. Bishop et al. (2002) carried out a direct study of the effects of dust input into the Sub-Arctic North Pacific, which showed a biotic response to the natural iron fertilization resulting from the input of Gobi Desert dust in April 2001. Observations of particulate organic carbon (POC)/chlorophyll systematics strongly supported an iron fertilization effect. A recent careful study (Wells, 2003) of the chemical speciation suggests that soluble iron concentrations need only increase slightly ($\leqslant$25 pM) above ambient levels for large diatoms to grow rapidly. It is likely, then, that very small but continuous increases in iron

flux might still stimulate large diatom blooms in high-nitrate, low-chlorophyll (HNLC) waters. A similar conclusion also reached by Price and Morel (1990) was that even trace amounts of metals (Fe, Zn, Co, Ni, Cu and Cd) can be nutrients for algal growth in impoverished environments such as the oceans. However, several recent papers suggest that, while iron addition could stimulate phytoplankton growth, its impact on POC export is limited (Boyd et al., 2004; Buesseler et al., 2004; Coale et al., 2004). Other studies have demonstrated the dust fertilizing effect by correlating biomarker productivity with dust input proxies. Ikehara et al. (2000) report phytoplanktonic biomarker records (alkenones, dinosterol and brassicasterol) for the last two deglaciations from the Southern Ocean. Enhanced atmospheric transport of dust was linked synchronously to the increased marine productivity at the glacials, presumably due to the increased supply of iron. In another study, Calvo et al. (2004) used alkenone and sterol biomarkers to assess the community structure response to dust input in the Tasman Sea as inferred from *n*-alkane fluxes during the last 470 kyr. The parallelism between brassicasterol and *n*-alkane fluxes was taken to indicate that diatom productivity responded to increased dust input during the glacials. Amo and Minagawa (2003) reported TOC and biomarker data for the Shatsky Rise in the Western North Pacific over the last 130 kyr. They suggest that this dust input comes from the Chinese Loess Plateau (CLP) region. They quote the CLP dust as having about 3% iron and cite high inputs of aluminium and titanium during the LGM. Using TOC and biomarkers as paleoproductivity proxies, they conclude that 'the eolian dust supply played an essential role enhancing paleoproduction during the LGM'. In other studies, Henriksson et al. (2000) suggest that fine, iron-rich, dust fertilized growth of dimethyl sulfide (DMS) producers at site 167772 on the Equator in the South Atlantic during the glacial stages and Barcena et al. (2001) reported paleoclimatic data from a site in the Alboran (Med.) Sea, with high dust input and enhanced iron supply from about 22 to 10 ka.

1.4. Biomarkers and terrigenous input

The long chain *n*-alkanes (C_{27}, C_{29}, C_{31} and C_{33}) and *n*-alkanols (C_{24}, C_{26}, C_{28} and C_{30}) are specific to higher land plant leaf waxes (Eglinton and Hamilton, 1967) and are transported to marine sediments via eolian dust (Simoneit et al., 1977; Gagosian et al., 1981; Huang et al., 2000; Zhao et al., 2003) and fluvial particulate matter (Bird et al., 1995; Pelejero et al., 1999). The *n*-alkane content of surface sediments from the Kara Sea shelves has been used to estimate that 70% of the preserved organic carbon in that area is terrestrially derived (Fernandes and Sicre, 2000). Likewise, near surface sediments of the Dead Sea contain organic matter of mostly terrestrial origin (Oldenburg et al., 2000). In contrast, the same approach reveals a low terrestrial input on the continental slope of the Nansha Sea, China (Duan, 2000). Several studies have interpreted the stratigraphic variations in the *n*-C_{29} homologue (nonacosane) in terms of changing terrigenous input related to wind strength and dust input (Poynter et al., 1989b; Ishiwatari et al., 1994; Madureira et al., 1997; Cacho et al., 2000; Sicre et al., 2000; Zhao et al., 2000; Amo and Minagawa, 2003; Zhao et al., 2003; Calvo et al., 2004). Higher alkane content in the South China Sea during the last glacial was attributed to enhanced river input caused by lower sea level (Pelejero, 2003), but alkane maxima during the deglaciation in the Sea of Okhotsk were interpreted as a result of the outflow of terrestrial organic matter from the submerged continental shelf when the sea level rose (Seki et al., 2003). On the other hand, higher sedimentary *n*-alkane content in the N. Atlantic during glacial times has been attributed to terrigenous sediments transported by ice-rafted debris (Villanueva et al., 1997).

The long chain *n*-alkanols have been used similarly to evaluate terrigenous input into marine sediments (Poynter et al., 1989a; Cacho et al., 2000; Sicre et al., 2000; Sicre et al., 2001; Ternois et al., 2001). However, there are a few reports of the presence of some homologues (e.g., C_{22}–C_{28}) in microalgae and cyanobacteria, so a marine contribution to the sedimentary record is a possibility (Volkman et al., 1999). In addition, the relationship between the abundances of selected *n*-alkanes and *n*-alkanols has been evaluated first as the HPA Index (Poynter and Eglinton, 1991), and more recently as the Alcohol Index (AI; Cacho et al., 2000). In the western Mediterranean Sea, lower AI values have been ascribed to preferential mineralization of the *n*-C_{26} alkanol due to increased deep water ventilation, consistent with a stronger northern hemisphere wind system (Cacho et al., 2000).

1.5. Preservation of organic matter and opal and productivity estimation

The most important uncertainty underlying the use of productivity proxies is that of production vs. preservation (Calvert and Pedersen, 1992). The sedimentary content of TOC and of individual organic compounds (Prahl et al., 1989) is influenced by a variety of biogeochemical factors, notably primary productivity, water column remineralization, sedimentation rate and bottom water oxygen concentration and exposure time (Eppley and Peterson, 1979; Mueller and Suess, 1979; Pedersen and Calvert, 1990; Hedges and Keil, 1995; Tyson, 2001). Only a small proportion (often less than 1%) of the original surface production is preserved in the sediments (Suess, 1980; Romankevich, 1984). Hence, it is often debatable whether the sedimentary organic content mainly reflects surface productivity or the efficiency of preservation. For preservation, there is also some uncertainty regarding the role of the redox condition of the surface sediments (Pedersen and Calvert, 1990; Hartnett et al., 1998; Hoefs et al., 2002; Sinninghe Damsté et al., 2002; Hartnett and Devol, 2003) versus sedimentation rate (Tyson, 2001) as the central factor.

After studying chlorins in sediments on the Oman margin in the Arabian Sea, Shankle et al. (2002) decided that they can be regarded as indicators of palaeoproductivity, though the controls are complicated in terms of water depth, bottom water oxygen levels and sediment grain size. The chlorin signal depends on the local depositional environment as well as the surface production. They concluded that sedimentary chlorins can be used as a proxy for palaeo productivity with the reservation that the rate at which they are degraded is not well understood. Increased primary production results in higher chlorin concentrations reaching the sediment. Also, an increased sedimentation rate allows a higher proportion of the chlorin flux to be preserved. Prahl et al. (1989) reported biomarker records at MANOP site C in equatorial Pacific Ocean and concluded that absolute quantitative assessments of marine source contributions based on analysis of biomarkers are hampered by the same limitations as TOC, since only a small fraction is preserved in the sediments. They suggested that combined methods are needed to separate production from preservation effects. Other recent studies find that production is the dominant factor in controlling the downcore organic records (Hinrichs et al., 1999; Schouten et al., 2000). Hinrichs et al. (1999) pointed out that the alkenones, diols, and the long chain fatty acids belong to the most refractory group of biomarkers, which are less subject than other types of lipids to oxic degradation.

It is apparent that, with the diverse environmental conditions bearing on surface water productivity, water column processes, sedimentation, and early diagenesis/burial, it is unlikely that the content or MAR of any biomarker proxy can be used as an absolute productivity indicator. However, some of these environmental effects can be allowed for by comparing the relative downcore variations of several proxies (Versteegh and Zonneveld, 2002), especially if the sedimentation rate is relatively constant.

We conclude that sedimentary biolipids can be used to partially reconstruct the overlying marine phytoplankton community and the terrigenous inputs, but only with certain reservations. First, selective preservation is a major factor, but it is also evident that the relationship between the biomarkers and their original sources is not a simple one, just as it is with other types of proxy such as opal. The principal difficulty lies in establishing just which organisms have been responsible for the production of the biomarkers. Thus, with dinosterol, which of various species or even which genera of dinoflagellate actually produced this sterol and to what extent? In effect, what precisely does a change in the abundance of dinosterol within a core mean? Since different species of dinoflagellates have different environmental needs, such as depth in a water column, nutrient concentrations, etc. we really would wish to know which species has contributed. Instead, we have to make do at present with the generalization of a semi-quantitative contribution from dinoflagellates as a class or group of organisms.

The same considerations apply to all biomarkers, including the alkenones, which largely reflect only Emiliania and Gephyrocapsa productivity within the haptophytes. However, in the case of the alkyl diols, the limited literature data indicate that these compounds are made by the eustigmatophytes and, to a lesser extent, diatoms. We are unable to separate out the contributions from these organisms which have rather different environmental requirements and hence have adopted the eustigmatophyte/diatom assignment as a provisional working basis.

What emerges from these considerations is that there is clearly benefit to be obtained by surveying large numbers of individual species of organisms

for gene content. It should be possible to arrive at more firmly based interpretations of sedimentary biomarker abundances when the key genes for the formation of these lipids have been located, identified and surveyed in the biosphere and in type environments. Closer links should then be apparent between biomarkers and the environmental conditions under which they are formed.

The environmental controls on opal production and dissolution in both the water column and sediments have been documented extensively (Ragueneau et al., 2000). The authors concluded that the efficiency of biogenic silica export fluxes, lateral advection of water masses, sediment redistribution, and spatial variations in the preservation efficiency of the biogenic silica all affect the use of opal as a productivity proxy. For example, lower opal export rate in the Atlantic Ocean than the Pacific Ocean could partially explain the lower opal content in the Atlantic Ocean sediment. They hypothesized that the low ambient silicic acid concentration in waters off NW Africa could induce the growth of diatoms more susceptible to dissolution, which would further decrease their export rate. On the other hand, opal flux does not change significantly with depth in the deep water, but sedimentary processes do. For our site, glacial–interglacial timescale changes in silica supply brought by dust and upwelling of different water masses should affect opal preservation efficiency.

1.6. The site

Site 658 lies directly beneath an area of permanent upwelling mostly controlled by the strength of the northeast trade wind (NETW); it is in the central region of dust deposition, supplied by the Saharan air layer (SAL) and the NETW (Figs. 1 and 2). Upwelling of nutrient-rich waters and fertilization by eolian dusts enhance productivity in the photic zone at this site relative to the open ocean, resulting in high sedimentation rates estimated at 10–20 cm kyr^{-1}, and total organic carbon contents of up to 3% (Harris et al., 1996). The site has been the focus of a number of investigations regarding the evolution of both the marine and terrestrial paleoenvironments of the region over the last 500 kyr. Terrestrial records indicate long term increased aridity of the Sahara (Tiedemann et al., 1989), but humid periods also occurred abruptly (de Menocal et al., 2000). For the marine environment, glacial instability was revealed by abrupt changes in SST (Eglinton et al., 1992; Zhao et al., 1995). Marine productivity estimation generally revealed peaks at terminations (Harris et al., 1996; Higginson, 2000; Zhao et al., 2000).

Phytoplankton productivity at these latitudes is mainly controlled by the nutrient concentration, as supplied by several processes including the upwelling of deep and nutrient-rich waters, eolian dust deposition and fluvial flux. As a result, primary productivity is basically high for ODP Site 658, while its variability is determined by the climatic and oceanographic processes that influence the delivery of these nutrients to the surface waters. The supply of nutrients is firstly determined by the intensity of upwelling, which is primarily driven by the NETW strength (Fig. 1A). The upwelling cell off NW Africa (Fig. 1B) generates surface waters which are amongst the most productive in the oceans. The Late Quaternary trade wind history has been estimated mainly by analyzing eolian terrigenous material (Sarnthein et al., 1982) and pollen (Hooghiemstra, 1989) in the sediments, and it was generally concluded that the glacial wind was stronger than that of the interglacial. However, recent studies show that productivity peaks were associated with terminations for this region and for regions further north in the Atlantic (Bertrand et al., 1996; Harris et al., 1996; Thomson et al., 2000; Zhao et al., 2000; Moreno et al., 2002). The higher productivity during the terminations suggests stronger upwelling, associated with the interaction of atmosphere and ocean circulations, SST changes and melt-water discharges (Thomson et al., 2000; Moreno et al., 2002).

Also important was the nutrient level of the upwelled water, which is mainly determined by the paths and strengths of the deep sea circulation (Higginson, 2000). Upwelling can only result in new production if the inventory of nutrients, new and recycled, is sufficient to sustain it. The quantitative balance between new and recycled nutrients needs more attention. Presently, ocean circulation off NW Africa involves four water masses: North Atlantic Deep Water (NADW) flows southwards below 2000 m from the North Atlantic, resulting in low-oxygen bottom waters around Cap Blanc (Sarnthein et al., 1982; Futterer, 1983). NADW flow was reduced during peak glacial cooling, replaced at least in part by northward-flowing nutrient (e.g., nitrate)-rich, corrosive Antarctic Bottom Water, flowing north along the western continental margin. Above this, highly saline and more oxygen-rich

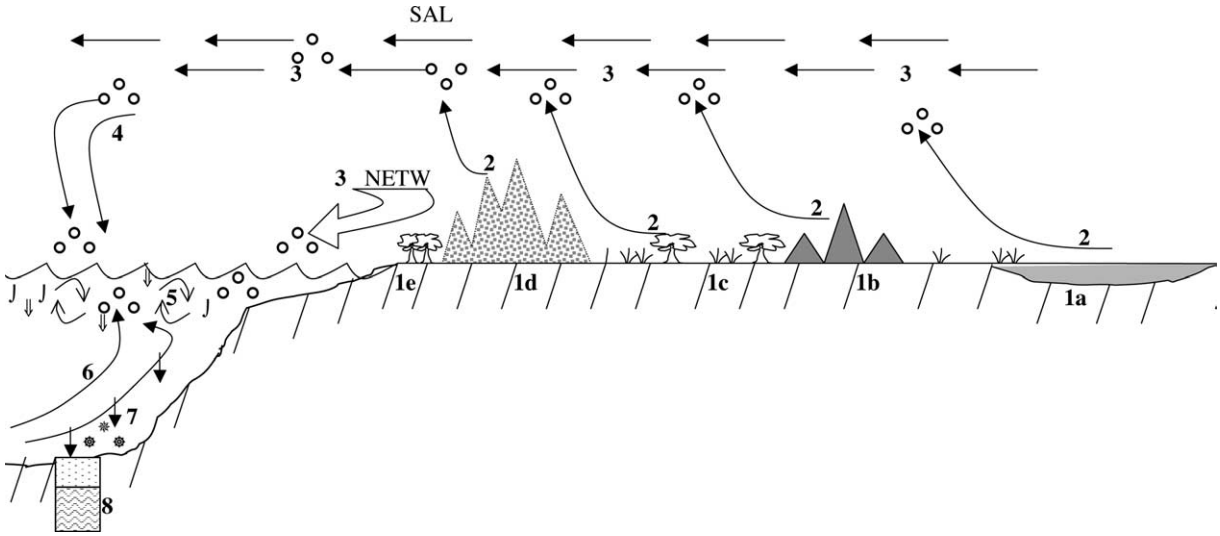

Fig. 2. Schematic of sources and ablation and transport systems supplying dusts from NW African continent to the photic zone at Site 658 off Cap Blanc in the NE Atlantic.

1. *Major dust sources*
   (1a) The Lake Chad Basin, including the Bodele depression (ca. 14°N, and 15°E)
   (1b) The Central Saharan mountain massifs of Ahoggar, Air, and Tibesti.
   (1c) The transcontinental Sahel zone running West to East to the South of the Sahara.
   (1d) The North and Western region encompassing arid parts of Morocco, Algeria and Mauretania in the peri-mountain regions to the North of the Sahara.
   (1e) The Mediterranean and North West coastal zones.
2. *Dust ablation*
   Lift off of dust and fine soils is very dependent on aridity. Dust flux to the NE Atlantic can be expected to be low in pluvial episodes, and high in cold, arid and windy times.
3. *Dust transport*
   Dust lifted off during storm events is transported at ca. 3–5 km height, mainly by the SAL, from East to West across the Sahara to the Atlantic.
4. *Dust fall out and rain out*
   Dust fall out from the transiting dust clouds brought by the SAL and the NETW occurs fairly continuously but maximizes in rain storms. Dust supplies both macro- and micro- mineral nutrients.
5. *Photic zone processes*
   The photosynthetic zone, the top tens of meters, is comprised of cold upwelling water masses containing macronutrients. Loss of nutrients occurs through dispersion by surface currents and the rain of fecal debris to the ocean floor.
6. *Upwelling of ocean waters*
   At Site 658, the upwelling is driven by the NETW, modified to some extent by the upper air flows of the SAL, bringing cold mid-water masses to the surface. At present, these are mainly NADW, rich in macronutrients such as nitrate and phosphate.
7. *Sedimentation through the water column*
   Ballasting by the heavy eolian particles, ingested by zooplankton and excreted in fecal pellets, speeds the descent of organic debris. The mineral particles also adsorb and physically protect organic matter.
8. *The sedimentary record*
   This combined regime of upwelling and eolian input is expressed as a high sedimentation rate of marine and terrigenous matter, both inorganic and organic.

Mediterranean outflow water (MOW) constitutes a significant flow from the north. Although restricted during glacially lowered sea level, the incursion of MOW during interglacial periods such as the Holocene has confined NADW flow to depths well below ~1750 m. Above the MOW, between ca. 150–400 m, low oxygen, nutrient-rich South Atlantic Central Water (SACW) separates deep water flow

from the sluggish, wide and shallow eastern boundary current, the Canary Current (CC) above. The CC, the southward limb of the Portuguese current, originates from the North Atlantic Drift and flows along the Iberian and N. African continental margins, where it becomes gradually detached from the continental slope between 25°N and 21°N due to low-level wind forcing (Gabric et al., 1993). This current may have transmitted cold meltwaters during ice rafting events in the North Atlantic (Zhao et al., 1995).

The riverine input is known to bring in nutrients, such as dissolved silica which can be expected to enhance diatom production and preservation. However, the particulate load is not normally carried far out to sea, and its contribution to the ballasting effect is not expected to be significant at this site. More importantly, significant amounts of nutrients can be brought to the coastal region by the flooding of continental shelves during the deglaciation (Bertrand et al., 1996; Thomson et al., 2000).

As reviewed in Section 1.3, dust input can increase productivity. In addition, dust can also enhance organic preservation by two means. The first is its contribution to the rapid transport of organic production to the sea floor through the ballasting effect of mineral particles incorporated in fecal pellets (Ittekkot and Haake, 1990; Armstrong et al., 2002); the second is the contribution made to sedimentation rate which leads to the more rapid burial of organic matter (Fig. 2.7). The overall result is that an increased proportion of organic production can reach the sea floor, largely escape benthic processes and bioturbation and, hence, contribute to higher TOC and biomarker contents in the benthic sediments (Fig. 2.8).

1.7. Approach and goals

Multi-biomarker analyses from the same core offer increased scope for evaluating variations in both total and individual phytoplankton productivity, and this approach has been applied routinely to reconstruct paleocommunity structure change in a variety of climate settings (Schubert et al., 1998; Hinrichs et al., 1999; Versteegh and Zonneveld, 2002; Menzel et al., 2003; Schulte and Bard, 2003; Higginson and Altabet, 2004).

We report here new molecular abundance data for alkenones, alkyl diols, dinosterol and *n*-alkanols at Site 658 for the last 160 kyr. These are compared with previously reported data for contents of TOC, chlorins, opal and *n*-alkanes from the same site. Typical abundances of alkenones, diols, dinosterol and *n*-alkanols are in the range of $\mu g\ g^{-1}$, less than 0.01% individually and less than 0.05% for all biomarkers combined. However, lithogenic abundances of clay and quartz vary between 10% and 50% each across the same interval (Tiedemann et al., 1989). We circumvent this disparity by comparing differences between the proxy abundances and the timing of maxima/minima. Our approach is based on the assumption that the chlorins can be used as a proxy for total phytoplankton productivity and, correspondingly, opal for diatoms, dinosterol for dinoflagellates, alkenones for haptophytes, and alkyl diols for eustigmatophytes/diatoms. The aim is to evaluate the information given by these different, individual biomarkers as proxies for specific phytoplankton groups. Temporal coherences and differences among these proxies from the same location may shed new light on the fertilization effects of the different nutrient sources. In addition, multi-proxy analysis allows for some evaluation of the effects of degradation of biomarkers as productivity proxies (Versteegh and Zonneveld, 2002).

2. Materials and methods

2.1. Stratigraphy

Three holes (A, B, and C) were drilled at ODP 658. A "common" age-scale was established for these sites (Zhao et al., 2003). It gives an average sedimentation rate of approximately 15 $cm\ kyr^{-1}$ for the last 160 kyr. However, sedimentation rates vary widely from 8.6 to 73.7 $cm\ kyr^{-1}$ for the last 23 kyr, afforded by 13 AMS ^{14}C dates. For the interval of 23–160 ka, the age model was mostly based on the benthic isotope stratigraphy of 658A and B, and the sedimentation rate varied only between 9 an 20 $cm\ kyr^{-1}$. There was a hiatus in 658A/B from 8.8 mbsf (50 ka) to 9.1 mbsf (74.5 ka), so no data were available for this section, but there was a relatively complete recovery of sediments for this interval from Hole 658C. The adopted age scale for 658C, however, retains some uncertainties (1–3 kyr) since it relies mostly on the $\delta^{18}O$ records for 658A and B.

2.2. Methodology

More detailed methods for lipid analyses were given in Zhao et al. (1995). Sampling resolution

was generally 2–5 cm (150–300 yr). For biomarker measurements, ca. 0.5 g of freeze-dried sediment was extracted with organic solvent (dichloromethane/MeOH, 3:1) three times, after adding the internal standard containing C_{21} *n*-alkanol and C_{36} *n*-alkane. Quantification of lipid biomarkers was achieved by comparing individual peak areas with those of the internal standards. Over 900 samples were analysed, mainly for the chlorin content and the range of homologues of alkenones, *n*-alkanes, *n*-alkanols, alkyl diols and the sterol dinosterol. The following individual biomarkers were analysed: C_{37} ($C_{37:2}$, $C_{37:3}$ and $C_{37:4}$ methyl) alkenones and C_{38} ($C_{38:2}$, $C_{38:3}$ methyl and $C_{38:2}$, $C_{38:3}$ ethyl) alkenones, 1,15-C_{30} and C_{32} diols, dinosterol, C_{27}, C_{29}, C_{31} and C_{33} *n*-alkanes, C_{24}, C_{26}, C_{28} and C_{30} *n*-alkanols. For alkyl diols, a limited number of samples were analyzed using GC-MS as the TMSi ethers. The homologues and isomers were recognized by their relative elution order and fragmentograms (de Leeuw et al., 1981; Poynter, 1989; Poynter et al., 1989a). The C_{30} and C_{32}-1,15-diols were the most abundant with some C_{28} and C_{30}-1,14-diols also present. Biosynthetically related series of other compounds, such as the unsaturated alkyl diols, the hydroxy alkanones and the hydroxy alkanoates, were not studied. Under these analytical conditions for the total extracts as the TMSi ethers, the sterol region was not efficiently resolved, with the exception of the dinosterol peak. Hence, brassicasterol could not be accurately determined.

Analyses of chlorins (658C) were reported in Harris and Maxwell (1995), with sampling resolution of 150–300 yr per sample. Opal (658A/B cores) was measured by Tiedemann (1991) using sliced cores, with resolution of only approximately 2000 yr per sample.

Conversion of the contents of the various parameters to their MARs was achieved using the following formula (Tiedemann et al., 1989):

$$\mathrm{MAR} = \mathrm{LSR} \times \mathrm{DBD} \times C,$$

where MAR is in $\mu g\ cm^{-2}\ kyr^{-1}$ for the biomarkers, and $g\ m^{-2}\ yr^{-1}$ for TOC and opal, LSR is the linear sedimentation rate ($cm\ kyr^{-1}$), DBD is the dry bulk density ($g\ cm^{-3}$ wet volume), *C* is the sediment component content ($\mu g\ g^{-1}$ for biomarkers and wt% for TOC and opal). Since DBD was not determined for 658C, we used the data from 658A/B for the same composite depth (Tiedemann et al., 1989). Sedimentation rate is calculated based on the "common" age-scale.

3. Results

Fig. 3 presents the contents and MARs of TOC, chlorins, opal, $\Sigma C_{30} + C_{32}$ diols, $\Sigma C_{37} + C_{38}$ alkenones, dinosterol and Σ*n*-alkanes and *n*-alkanols, as well as the linear sedimentation rate (LSR) for the last 160 kyr. The SST record (Fig. 3H) has been reported (Zhao et al., 2003), but is included here for comparison purposes. The contents of TOC, chlorins, opal, C_{37} alkenones and *n*-alkanes have been reported previously (Tiedemann, 1991; Harris and Maxwell, 1995; Harris et al., 1996; Jordan et al., 1996).

TOC content (Fig. 3A) varied between 0.5% and 3%, with values generally higher during the warm stages (MIS 5, 3 and 1) and lower during the cold stages (MIS 6 and 2). However, the cold MIS 4 showed two large oscillations, with values reaching 3%.

Chlorin content (Fig. 3B) shows variations from 1 to 18 $\mu g\ g^{-1}$. Higher values and maxima are observed around 0–4, 8–15, 33–50, 60–67, and 123–133 ka, lower values and minima occurred around 8, 15–30, 50–60, 135–150 ka. Generally, peak glacial periods of LGM (23–18 ka) and PGM (145–135 ka) had lower chlorin values, but the amounts for MIS 4 were high. Deglaciations and MIS 3 had higher values, but most of MIS 5 (70–120 ka) had low values.

Opal content for 658A and B (Fig. 3C) ranged from 2% to 33% with two peaks centered at the deglaciation (11 and 128 ka, respectively). The lowest values were near the LGM and PGM. There were no data for MIS4 due to the hiatus.

The C_{30} and C_{32} alkyl diols (Fig. 3D) show similar downcore variation and the *X*–*Y* plot yields a correlation coefficient (R^2) of 0.86 (Fig. 4A), in agreement with the assumption that they have common sources. The total contents of the C_{30} and C_{32} alkyl diols, range from 0.3 to 14 $\mu g\ g^{-1}$. Higher values and peaks are recorded for example, at 0–4, 10–15, 30, 37–44, 60–67, 115, 122–132 ka. Lower values and some minima are recorded at, for example, 4–10, 15–27, 50–60, 83–85, 117–122, 132–142 ka. There are no clear glacial to interglacial patterns, except that the two peak glacial periods (LGM and PGM) both had very low values.

C_{37} and C_{38} alkenones (Fig. 3E) show almost identical downcore profiles and an R^2 of 0.98 in an *X*–*Y* plot (Fig. 4B), in accordance with their common sources. Total alkenone values vary by a factor of 32 (1–32 $\mu g\ g^{-1}$). Higher values and peaks are observed around 0–4, 38–45, 60–80, 85–92,

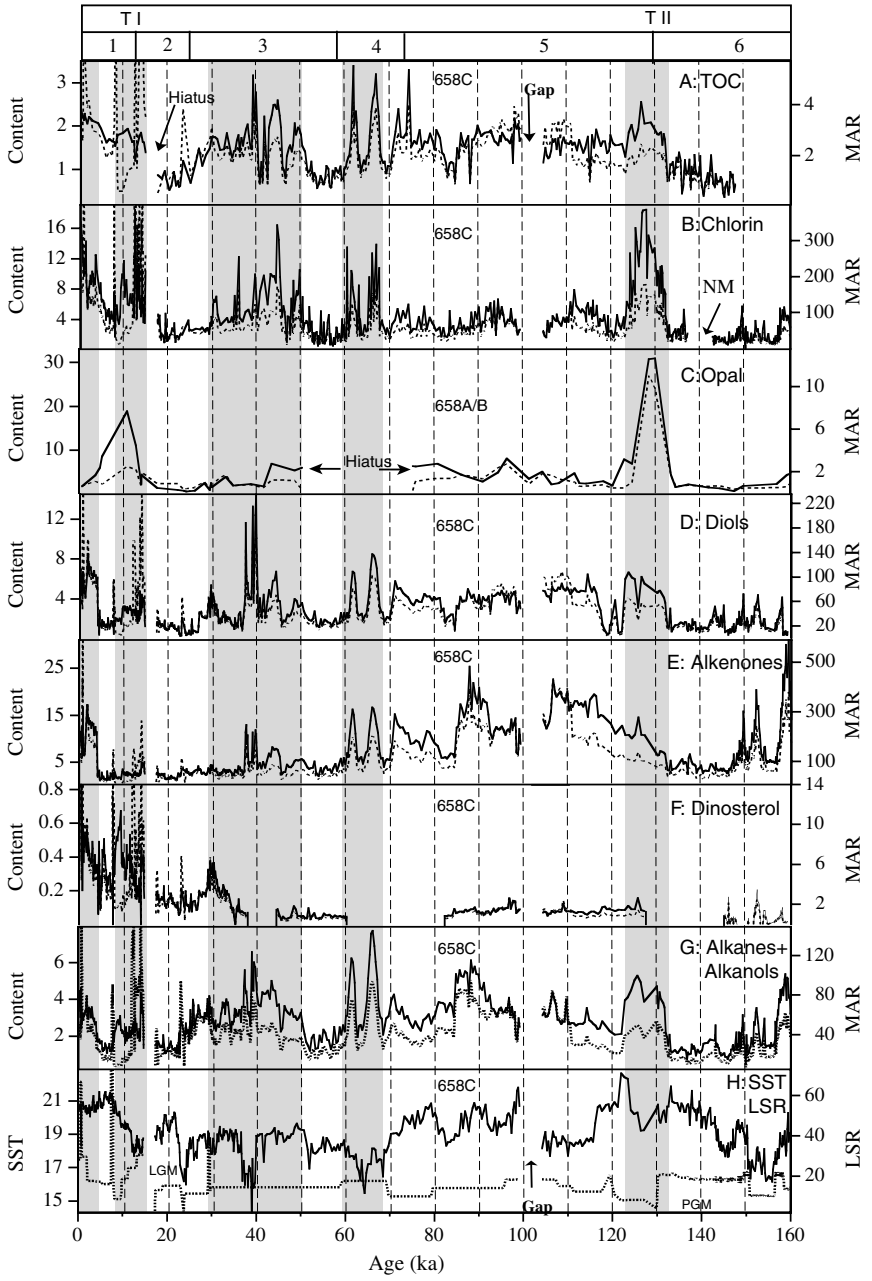

Fig. 3. Content and MAR records for ODP Site 658C over last 160 kyr, together with records for biogenic opal for 658A and B and $U_{37}^{K'}$ SST and linear sedimentary rate data for 658C. Marine isotope stage boundaries (1–6) are labeled on the top. LGM is the last glacial maximum and PGM is the penultimate glacial maximum and T1 and T2 indicate Terminations. The arrow labeled Gap is for a coring gap between 99.1 and 104.3 ka in 658C. Solid lines are for content and dashed lines are for MAR. NM is 'not measured'. (A) Content (%) and MAR ($g\,m^{-2}\,yr^{-1}$) of TOC. (B) Content ($\mu g\,g^{-1}$) and MAR ($\mu g\,cm^{-2}\,kyr^{-1}$) of chlorins (Harris et al., 1996). (C) Content (2–63 μm fraction, carbonate-free, %) and MAR ($g\,m^{-2}\,yr^{-1}$) of biogenic opal for ODP 658A/B (Tiedemann, 1991). (D) Content ($\mu g\,g^{-1}$) and MAR ($\mu g\,cm^{-2}\,kyr^{-1}$) of of $\Sigma C_{30} + C_{32}$ diols. (E) Content ($\mu g\,g^{-1}$) and MAR ($\mu g\,cm^{-2}\,kyr^{-1}$) of $\Sigma C_{37} + C_{38}$ alkenones. (F) Content ($\mu g\,g^{-1}$) and MAR ($\mu g\,cm^{-2}\,kyr^{-1}$) of dinosterol. (G) Content ($\mu g\,g^{-1}$) and MAR ($\mu g\,cm^{-2}\,kyr^{-1}$) of $\Sigma C_{27} + C_{29} + C_{31} + C_{33}$ *n*-alkanes plus $\Sigma C_{24} + C_{26} + C_{28} + C_{30}$ *n*-alkanols.

105–125, 147–160 ka, lower values and minima occurred around 5–37, 50–60, 132–147 ka. Alkenone content was generally higher during interglacials, but lower during glacials with the exception of higher values during MIS 4 and early MIS 6. The two peak glacial periods (LGM and PGM) and the two

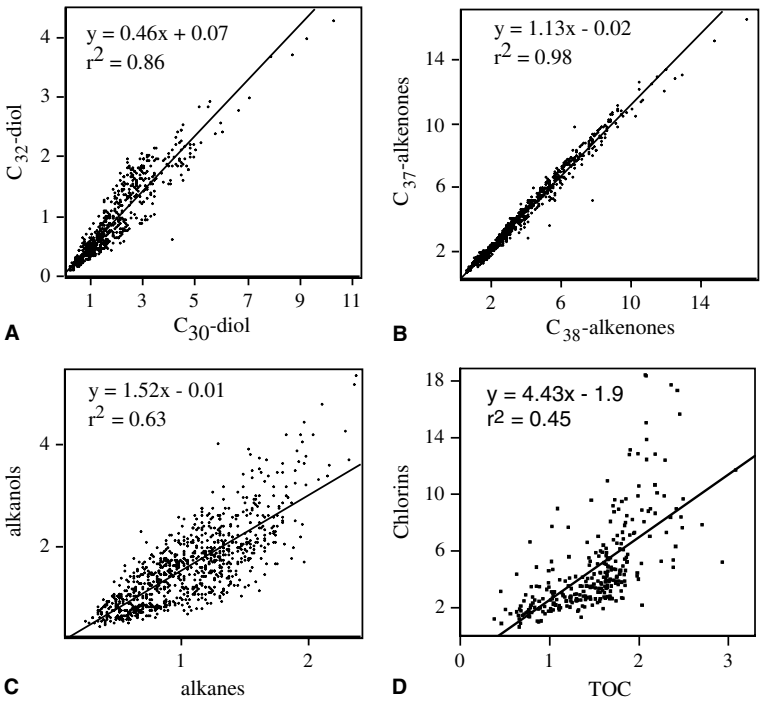

Fig. 4. *X–Y* plots of biomarker contents. (A) Content of C_{30} (μg g^{-1}) versus C_{32} alkyl diols (μg g^{-1}) (R^2 of 0.86). (B) Content of C_{38} (μg g^{-1}) versus C_{37} alkenones (μg g^{-1}) (R^2 of 0.98). (C) Content of $\Sigma C_{27} + C_{29} + C_{31} + C_{33}$ *n*-alkanes (μg g^{-1}) versus $\Sigma C_{24} + C_{26} + C_{28} + C_{30}$ *n*-alkanols (μg g^{-1}) (R^2 of 0.63). (D) Content of TOC (%) versus chlorins (μg g^{-1}) (R^2 of 0.45).

deglaciation intervals all had very low values, and the low values extended to the early Holocene for termination I. Interesting features are the persistent low alkenone concentration from 37 to 5 ka and the higher values in MIS 5.

Dinosterol content (Fig. 3F) shows a range of 0.03–1.5 μg g^{-1}. The content for several intervals (e.g., 37–44, 61–82 and 130–144 ka) was below detection limit, which was estimated at 0.02 μg g^{-1}. The content for the last 35 kyr was much higher than for the rest of the record. Within this interval, the LGM period had the lowest values. Dinosterol content increased at the start of deglaciation (15 ka) and reached a peak at around 9 ka, followed by some decreases at 7 and 4 ka. For the interval of 40–160 ka, dinosterol values were generally low. The glacial periods of MIS 6&4 had values below detection limit.

The *n*-alkanes and *n*-alkanols (Fig. 3G) show similar downcore profiles and an R^2 of 0.63 in an *X–Y* plot (Fig. 4C), in agreement with the assumption that they are both derived from land plant leaf wax. Their total content varied by a factor of approximately 5 for both groups. These terrigenous components seem to show slightly more variability than the marine derived organic components (chlorins, alkenones, dinosterol and diols; Fig. 3). Their contents do not demonstrate a clear glacial/interglacial pattern, but peak glacial times (LGM and PGM) did show lower values.

The MAR variations (Fig. 3A–G) generally parallel those of the contents of the same parameters, except for the last 15 kyr. Three significant MAR peaks are apparent at 14.7–13, 7.9–7.4 and 2–0.8 ka. On the other hand, the MARs are conspicuously low for all parameters for the interval 11.2–9.7 ka. These major deviations in MAR from contents are largely a result of variations of linear sedimentation rate (LSR, Fig. 3H) afforded by the 10 AMS ^{14}C dates for the last 15 kyr. Thus, sedimentation rate varies by more than a factor of 8 (8.6 cm kyr^{-1} for 7.9–9.7 ka to 73 cm kyr^{-1} for 7.9–7.4 ka) for this interval. For the interval of 23–160 ka, the age model was mostly based on the benthic isotope stratigraphy of 658A and B, and the estimated sedimentation rate varied only by a factor of 2 (between 9 and 20 cm kyr^{-1}). Thus, sharp increases or decreases in MARs are created at age control points even if there are no significant changes in the contents of these parameters.

4. Discussion

4.1. Downcore variations in the marine productivity proxies

Both content and MAR of biogenic components have been used as proxies for paleoproductivity. In view of the potentially sharp boundaries created by age control points, it is important to cross correlate both the MAR and content records of the same parameter.

Five intervals of higher total phytoplankton productivity are indicated by the chlorin content and MAR records. Two occurred during deglaciations or terminations (15–8 and 133–123 ka), one occurred during the late Holocene interglacial (4–0 ka) and one occurred during the milder intervals of the last glacial (50–30 ka), but only one occurred during the glacial period of MIS 4 (67–60 ka). The five intervals are termed the High Productivity Intervals (HPIs) of the Late Holocene, Termination I, MIS 3, MIS 4, and Termination II, for easier comparison. The opal record in 658A/B indicates only two major diatom productivity peaks at 15–8 and 133–123 ka that matched the two HPIs at the terminations well (Harris et al., 1996). There was a small opal peak during the early stage of the MIS 3 HPI, but opal content was very low for the late Holocene HPI. However, fewer peaks in the opal record may be a consequence of lower sampling resolution in 658A/B. No opal data were available for the MIS 4 HPI due to the hiatus in core 658A/B; hence, a major diatom peak may have existed between 75 and 50 ka. In addition, high productivity intervals were also identified for Terminations III and IV using total chlorin content (Higginson, 2000).

Alkyl diols show somewhat higher eustigmatophyte/diatom productivity during all five HPIs, although the Termination I peak was small. Of the 4 individual phytoplankton productivity proxies, the alkyl diol productivity record has the best match with the total productivity (chlorins) record. Alkenones revealed higher haptophyte productivity during the HPI of the Late Holocene and the MIS 4, but smaller productivity peaks during the MIS 3 HPI, and a smaller and delayed Termination II HPI. However, no Termination I HPI was observed. On the other hand, two major and broad alkenone peaks in MIS 5 (at around 92–85 and 115–105 ka) correlate with smaller increases in the total productivity record of chlorins. The dinosterol record revealed only two higher dinoflagellate productivity periods that match the Late Holocene and Termination I HPIs. There was also a small peak near the end of the MIS 3 HPI. However, dinosterol was below the detection limit during the MIS 4 HPI and part of the Termination II HPI.

The most striking behavioral feature of these biomarker proxies is that they all indicate lower algal group productivity for this site during the two peak glacial times (LGM, 25-18 ka and PGM, 145-135 ka). Lower total productivity during the LGM for this region has been reported before (Bertrand et al., 1996; Harris et al., 1996; Zhao et al., 2000), but the lower productivity during the PGM suggests that the causative phenomenon could have operated during all the peak glacial periods for this region, as indicated by chlorin analysis (Higginson, 2000). All proxies, except the alkenones, also reveal higher productivity at the two terminations, in agreement with results from this region, the North Canary Basin (Moreno et al., 2002), the Iberian margin (Thomson et al., 2000) and the western Mediterranean (Barcena et al., 2001). Higher productivity, especially of diatoms, within a major upwelling region during Terminations would be expected to drive down atmospheric pCO_2 (Higginson and Altabet, 2004) at precisely the time that ice core records indicate that pCO_2 was rising sharply.

4.2. Downcore variations in terrigenous biomarkers

The terrigenous biomarkers, the *n*-alkanes and *n*-alkanols (Fig. 3G), show trends which are remarkably similar to those of major portions of the chlorin and TOC records. Thus, they show high values for all five HPIs. One explanation for the parallelism between the *n*-alkanes and *n*-alkanols and the TOC records could be that terrigenous input was a significant contribution to TOC. However, low resolution studies have revealed that TOC was primarily of marine origin for this site (Stein et al., 1989). In addition, optical observations of organic matter (OM) at nearby site 11K (for ca.last 60 Ka) reveal mainly structureless flakes, typical of a planktonic/bacterial origin, whilst continental OM (lignocellulose fragments) represents a minor contribution (Martinez et al., 1999). Rather, the most likely explanation lies in the fertilizing effect of the terrigenous input on the phytoplankton productivity, combined with enhanced preservation due to

increased sedimentation. The primary relationship must be between the *n*-alkanes and the *n*-alkanols reflecting terrigenous input and the chlorins representing total phytoplankton productivity. In general, colder and drier climates are associated with stronger winds and higher dust inputs (Tiedemann et al., 1989), but *n*-alkane and *n*-alkanol inputs may not always reflect dust inputs. Indeed, peak glacial times (LGM and PGM) had strikingly lower *n*-alkane and *n*-alkanol inputs for this site, which may reflect lower densities of vegetation cover of the dust source region at these cold and arid times (Zhao et al., 2003).

4.3. Downcore variations in TOC-normalized productivity proxies

One problem associated with using sedimentary biomarker contents as productivity proxies is that biomarkers are only a very small fraction of the total sediment contents, but lithogenic components can vary between 40% and 70% (Tiedemann et al., 1989; de Menocal et al., 2000; Zhao et al., 2003). Since both aridity and wind strength maximized at the LGM and PGM, it is likely that deflation and hence lithogenic flux also reached maxima at these times (Tiedemann, 1991; Ruddiman, 1997; Zhao et al., 2003). Therefore, lithogenic dilution of sediments could account in part for the lower biomarker contents during the LGM and PGM. However, sedimentation rates were about average (13–15 cm kyr^{-1}) during the LGM, but much higher during the deglaciation (30 cm kyr^{-1}) and part of the early Holocene (up to 73 cm kyr^{-1}). Indeed, comparisons of biomarker contents and MARs further confirm that productivity was the lowest during the LGM.

Another means of evaluating the productivity proxies is to normalize the contents to TOC in order to eliminate the dilution effects; these data are plotted in Fig. 5B–G. The TOC-normalized values generally show downcore variations paralleling those of the contents. We can deduce two preliminary conclusions. The first is that sediment dilution was not mainly responsible for the downcore variations. The second is that the downcore variations in the marine proxies were largely independent of TOC variability. This supports earlier arguments that biomarker variability is mainly controlled by surface productivity.

However, preservation must be considered (Calvert and Pedersen, 1992). As indicated above, environmental effects on preservation can be allowed for by comparing the relative downcore variations in several proxies (Versteegh and Zonneveld, 2002), especially if the sedimentation rate is relatively constant. At ODP site 658, the sedimentation rate for most of the record varied by only a factor of 2 over the last 160 kyr. The downcore variation in the marine biomarkers varied by up to a factor of 15 while terrigenous biomarkers varied by a factor of 5. Furthermore, the different marine biomarkers show peaks at different intervals. These results suggest sedimentation and diagenesis rates are not the main controls of the downcore variations of these biomarker contents at Site 658. The decreasing dinosterol content with increasing sediment age (Fig. 3F) does reveal a trend consistent with a strong preservational artifact for this record. However, a longer but lower resolution dinosterol record from 658A showed that dinosterol had many other high abundance peaks during the last 500 kyr, suggesting that surface production was also important (Poynter et al., 1989a).

We conclude that preservation alone does not explain the behavior of the biomarker productivity proxies in ODP 658C, though it will have played a role in controlling the magnitudes of their maxima and minima. Rather, we argue that their downcore variations mainly reflect primary production changes.

4.4. Principal component analysis and fertilization off the coast of NW Africa

The records of the productivity and the terrigenous input proxies (Fig. 3) clearly show similarities, but there are also major differences. Principal component analysis (PCA, Table 1) was performed using the JUP Program of SAS on the original content data of the proxies in order to highlight the commonalities and differences among the various measurements. In addition to the six direct productivity proxies (TOC, chlorins, opal, alkenones, dinosterol and alkyl diols), we also included $U^{K'}_{37}$ SST as it is related to upwelling, and alkanes and alkanols content as a proxy for terrigenous biomarker input. The first four factors account for 85% of the total variance of the data sets. Factors 1, 2 and 4 are all related to marine phytoplankton productivity, as each is loaded by one or more of the productivity proxies. Since factor 1 is loaded significantly by both TOC and chlorins, it is most likely the best total productivity indicator. For

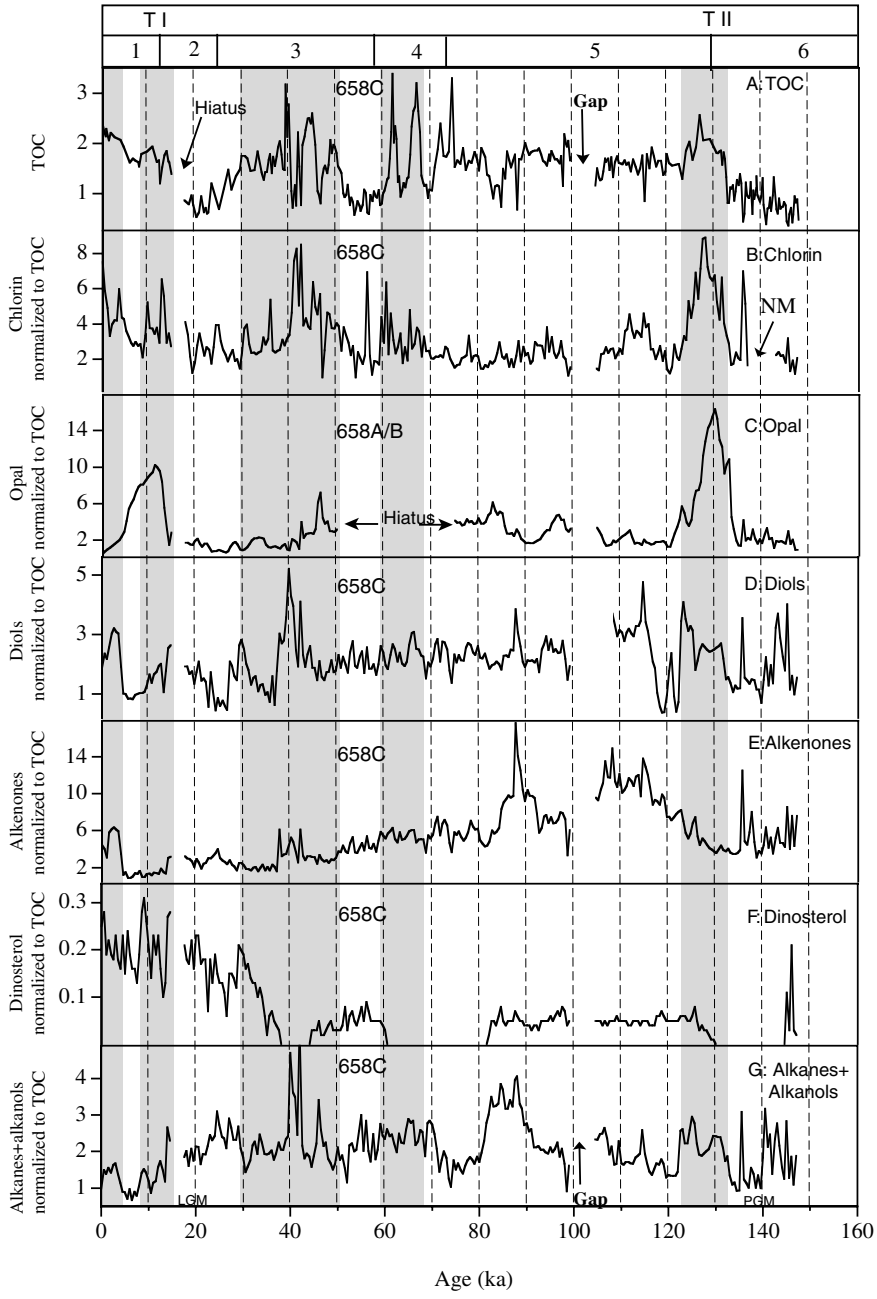

Fig. 5. Content of TOC and TOC-normalized contents of the other proxy records for ODP site 658 over the last 160 kyr. Marine isotope stage boundaries are labeled on the top. LGM is the last glacial maximum and PGM is the penultimate glacial maximum. The arrow labeled Gap is for a coring gap between 99.1 and 104.3 ka in 658C. (A) Content (%) of TOC. (B) Normalized content of chlorins (μg g^{-1} over % TOC). (C) Normalized content of biogenic opal for ODP 658A/B (% over % TOC for 658C). (D) Normalized content of $\Sigma C_{30} + C_{32}$ diols (μg g^{-1} over %TOC). (E) Normalized content of $\Sigma C_{37} + C_{38}$ alkenones (μg g^{-1} over %TOC); (F) Normalized content of dinosterol (μg g^{-1} over %TOC); (G) Normalized content of $\Sigma C_{27} + C_{29} + C_{31} + C_{33}$ *n*-alkanes plus $\Sigma C_{24} + C_{26} + C_{28} + C_{30}$ *n*-alkanols (μg g^{-1} over % TOC).

individual groups of phytoplankton, factor 1 represents mostly the productivity contributions from eustigmatophytes (diols) and haptophytes (alkenones) with some contribution from diatoms (opal), but no contribution from dinoflagellates (dinosterol). Factor 2 represents productivity con-

Table 1
Principal component analysis of data for core 658C and 658A and B (opal only)

	Eigenvalue	% of variance	Cumulative % of variance
Factor 1	3.43	42.8	42.8
Factor 2	1.48	18.5	61.3
Factor 3	1.00	12.5	73.8
Factor 4	0.93	11.6	85.3

Eigenvectors	Factor 1	Factor 2	Factor 3	Factor 4
TOC	0.477	0.106	0.042	0.161
Chlorins	0.406	0.400	0.001	−0.102
Opal	0.243	0.466	0.056	−0.614
Alkenones	0.342	−0.476	0.120	0.187
Dinosterol	0.047	0.546	−0.090	0.730
Diols	0.477	−0.182	0.005	0.099
SST	−0.059	0.069	0.986	0.069
Alkanes and alkanols	0.446	−0.220	−0.035	−0.062

Percentage of variance of the first four factors and the loadings of the proxies on factors 1–4.

tributions mainly from dinoflagellates and diatoms. The significantly negative loading of alkenones indicates that, at least for some time intervals, the productivity of haptophytes was lower when those of dinoflagellates and diatoms were higher. Factor 4 represents some additional productivity contributions from dinoflagellates and haptophytes, which occur when diatom productivity was lower. These results suggest temporal variations in phytoplankton community structure responding to environmental changes. The significant loading of the *n*-alkanes and *n*-alkanols in factor 1 reflects the visual observation that there are some strong similarities downcore between the records of the *n*-alkanes and *n*-alkanols and those of the productivity proxies. However, *n*-alkanes and *n*-alkanols are not produced by marine phytoplankton. Hence, their high loading in factor 1 supports the claim that the dust input which mostly carries them contributes significantly to the fertilization of the ocean phytoplankton (eustigmatophytes, haptophytes and diatoms), as well as enhancing organic preservation due to increased sedimentation. However, increased dust input during the LGM (Tiedemann et al., 1989) did not increase productivity (Fig. 3). One possible explanation is that the weakened upwelling (Zhao et al., 2000) did not bring up sufficient macronutrients to sustain the enhanced productivity for this site. Future studies using biomarkers and independent estimates of ocean nutrients by nitrogen isotope and carbon isotope measurements (Altabet et al., 2002) could help to clarify the situation regarding dust fertilization. Furthermore, as the terrestrial *n*-alkanes and *n*-alkanols are typically associated with the fine particles, they could be easily moved about by resuspension and lateral sediment transport caused by deep water flow (McCave, 2002). Hence, increased *n*-alkanes and *n*-alkanols in the core might not reflect higher dust input at the site. SST is the only significant loading on factor 3, accounting for 12.5% of the variance. Surprisingly, SST has no significant loading on factors 1, 2 and 4 (all productivity factors), indicating that upwelling is not one of the main causes of productivity variation at this site. If it were, we would expect a high negative loading of SST on at least one of productivity factors since stronger upwelling would enhance surface productivity but decrease SST (Hinrichs et al., 1999). We infer that the persistence of the upwelling cell has provided the basic scenario maintaining the high productivity, but that fertilization-induced variations in productivity have resulted from changing inputs of nutrients brought in by remote water masses and by eolian dust.

The correlations of these different proxies are further illustrated by the coefficients derived by multivariate analysis (Table 2). TOC and chlorins have a coefficient of 0.67 (Table 2 and Fig. 4D), which is in accord with the conclusion that most of the TOC is of marine origin (Stein et al., 1989). In fact, this correlation for ODP 658C was cited as the evidence that chlorins could be used as a paleoproductivity proxy (Harris et al., 1996). Among the individual phytoplankton productivity proxies, opal and diols reveal good correlation with chlorins, but alkenones do not. Opal and diols also do not correlate well. This is surprising,

Table 2
Multivariate analysis of data for core 658C and 658A and B (opal only) and cross-correlation coefficients

	TOC	Chlorins	Opal	Alkenones	Dinosterol	Diols	SST
Chlorins	0.667						
Opal	0.352	0.558					
Alkenones	0.466	0.172	−0.034				
Dinosterol	0.215	0.260	0.062	−0.165			
Diols	0.718	0.533	0.215	0.644	−0.008		
SST	−0.039	−0.044	0.001	−0.017	0.003	−0.097	
Alkanes and alkanols	0.645	0.457	0.225	0.549	−0.110	0.721	−0.121

since it has been proposed that alkyl diols are produced by diatoms under high productivity (upwelling) settings (Sinninghe Damsté et al., 2003). One possible explanation is that opal dissolves easily in the Atlantic Ocean surface water (Ragueneau et al., 2000) and is a poor proxy for diatom productivity, except for very productive intervals, such as the two terminations. Alternatively, the comparison provides some support for our provisional assignment of eustigmatophytes as the main producers of the diols. The terrestrial biomarkers, alkanes and alkanols show reasonable correlation with chlorins. Interestingly, diols, alkanes and alkanols, and alkenones all correlate well with TOC. These correlations probably reveal some preservation effects, since these lipid biomarkers are all fairly resistant to degradation. They are often better preserved than TOC (Versteegh and Zonneveld, 2002), but chlorins are less well preserved. Table 2 reveals that SST does not have any significant correlation with the other proxies. We infer that, while upwelling has maintained high productivity for Site 658, it could not account for the productivity variations.

Another likely explanation for the observed patterns in biomarker and TOC contents may lie in changes of wind direction and seasonality during the glacials (Martinez et al., 1999). The intensification of offshore winds at the LGM (Shimmield, 1992; Leroux, 1993; Grousset et al., 1998; Martinez et al., 1999; Zhao et al., 2000) could have caused a persistent over-deepening of the mixed layer within the upper waters of the center of the upwelling cell. As planktonic species would have been consistently convected down to 40–50 m depth, essentially below the euphotic zone, it is possible that this could have resulted in relatively lower in situ marine productivity when offshore winds were most intense. Furthermore, light attenuation and surface water turbidity caused by the increased surface wind shear and maximum aerosol loading of near surface winds could have restricted phytoplankton production (Huntsman and Barber, 1977). Both of these effects have been observed during in situ studies of the most intense region of upwelling today (Huntsman and Barber, 1977; Gabric et al., 1993). Certainly, reconstructions of paleo-winds during peak glacials suggest more prolonged, intense winds, with intensified trade winds focused between the stationary ITCZ and a depressed paleo-polar front.

Other processes affecting the productivity at Site 658 and this region in general include the nutrients transported by eolian dusts and fluvial fluxes and the upwelling of the different water masses, which are reviewed in Sections 1.3 and 1.6, respectively. The relationships between these various fertilizing mechanisms must be complicated. While heightened wind speeds tend to increase both the dust input and the upwelling strength, hence summing the fertilizing effects, the situation is not simple (Fig. 2.5). For example, an increase in the speed of the higher altitude SAL may result in more dust being delivered to the ocean, but the SAL's effect on upwelling (Fig. 2.6) is likely to be small. River flux usually increases during the humid and warm interglacial stages, but its relationship with upwelling is not known. Thus, one would not expect to correlate the productivity record with the behavior of any single paleoclimatic or paleoceanographic proxy. It is the interplay of the different fertilizing agents that will determine the final appearance of the productivity record. Overall, for a site like 658, the basic picture would be that upwelling provides most of the macronutrients (such as nitrate, phosphate and dissolved silica), giving rise to high background productivity, while other nutrients, such as iron, are mainly supplied by eolian and other inputs from the continent (Fig. 2.5 and 2.6). Plankton stimulation is obviously related to the macronutrient inventory of the oceans, especially nitrate in waters supplying this upwelling cell (SACW, MOW and the CC). Specifically, since the

HPIs at the two terminations were mainly the result of increased diatom productivity, the increased fertilization was most likely induced by the riverine input of dissolved silica. On the other hand, for the MIS 4 HPI, peaks were evident in most of the productivity proxies (no opal data). Since this interval was also characterized by lower SST, nutrient supply was most likely caused by increased upwelling.

4.5. Changes in phytoplankton community structure on the geological timescale

A significant feature of the 658 biomarker records is that the alkenone content was low during the two HPIs indicated by high chlorin contents at the terminations (Fig. 3). These results and the PCA analyses seem to suggest that there is a degree of independence shown by the productivities of the major primary producers in this region of the ocean. For Termination II, during the transition from lower to higher total productivity, the algal productivity represented by the biomarkers started almost coevally with the diatoms and eustigmatophytes, followed by the dinoflagellates and then the haptophytes (Figs. 3 and 5). The slight leading of the diatom peak over the total productivity peak is likely caused by lower sampling resolution and by use of the 658A and B cores, rather than the 658C core, for the opal measurements. Similar but less obvious sequential trends are also observed for Termination I. Another means to seek out the temporal relationships between the individual phytoplankton groups and their contributions to total marine productivity is to normalize the various contents to chlorin content (Fig. 6). Peaks in each of these chlorin-normalized phytoplankton productivity proxies reflected relatively higher individual contributions to total productivity. However, interpretations based on the normalized contents need to be tentative as the amplitude variations often reflect more about the changes in chlorin content rather than of the other biomarkers. For example, chlorins display well-defined maxima at ca. 125, 113 and 90 ka, but diols, alkenones and dinosterol do not (Fig. 3). Again, the minima in the normalized contents of diols, alkenones and dinosterol at these times only indicate relative decreases in the respective phytoplankton groups as contributors to the total productivity. Nevertheless, these normalized proxy records allow us to assess which phytoplankton groups were the major contributors to each of the 5 HPIs. Thus, normalized opal peaks for Terminations I and II reveal increased diatom contributions to total productivity but low contributions for the MIS 3 and Late Holocene HPI. The chlorin-normalized alkyl diol record reveals small contributions of eustigmatophytes/diatoms to total productivity for Terminations I and II, but increased contributions to the MIS 4, MIS 3 and late Holocene HPI. On the other hand, the eustigmatophyte/diatom contribution was higher during MIS 5 when total productivity was lower. Haptophyte contributions had similar patterns to those of the eustigmatophytes/diatoms, with the highest values in MIS 5 when total productivity was lower. Both groups also reveal a decreasing trend from MIS 5 toward the Holocene. Dinosterol, on the other hand, reveals the opposite trend for the dinoflagellates, with increasing contributions toward the Holocene.

These phytoplankton community structure changes at Site 658 must reflect differening responses of the various phytoplankton groups to paleoenvironmental changes. Our results add to the literature evidence that phytoplankton community structures do change in particular regions of the oceans on geological timescales and that these changes are probably caused mainly by regional variations in the amounts and relative proportions of available nutrients. The mechanisms may involve the differing responses of the various types of phytoplankton to the changing supplies of both macro- and micronutrients. The eolian nutrients certainly include iron from the iron-rich rocks of the Sahara and this iron can be expected to make a major contribution to the elemental needs of phytoplankton (Boyd et al., 2000). Furthermore, many other micronutrients will be supplied from the different types of sediments eroded from the NW African Continent. Thus, opal and chlorin abundance peaks at the two terminations were most likely the result of increased diatom productivity, in response to increased riverine nutrient (especially silicate) input (Tiedemann, 1991; Martinez et al., 1999). For micronutrients, it has been demonstrated that diatoms and haptophytes require different trace metals to stimulate their growth (Morel et al., 1994). *E. huxleyi* has a Co requirement that could only be partly met by Zn, while the diatoms *Thalassiosira pseudonana* and *T. oceanica* have Zn requirements that could be largely met by Co (Sunda and Huntsman, 1995).

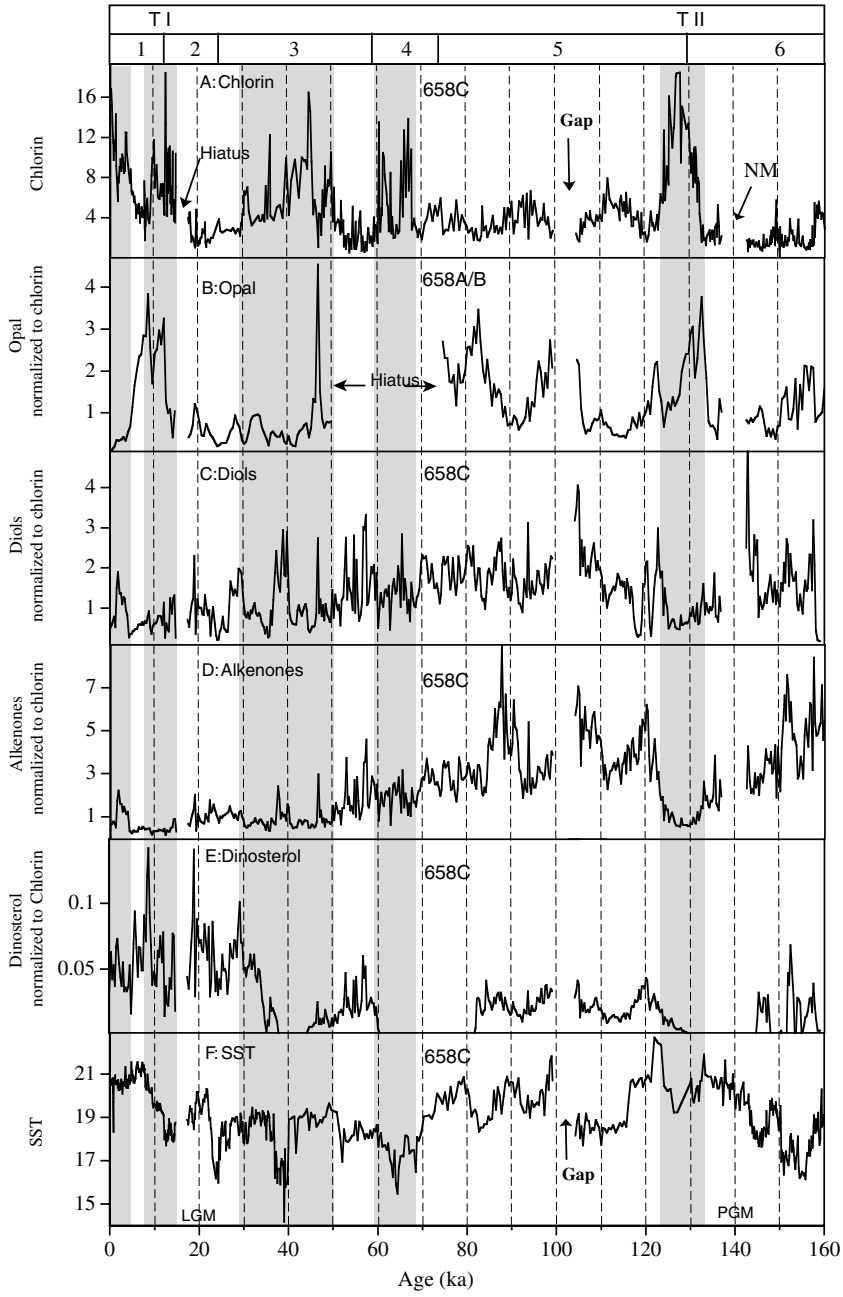

Fig. 6. Content of chlorins and the chlorin-normalized contents of the other proxy records for ODP Site 658 over the last 160 kyr. Marine isotope stage boundaries are labeled on the top. LGM is the last glacial maximum and PGM is the penultimate glacial maximum. The arrow labeled Gap is for a coring gap between 99.1 and 104.3 ka in 658C. The arrow NM indicates that chlorins were not measured for the interval of 137 to 142.5 ka. (A) Content of chlorins (μg g^{-1}). (B) Normalized content of biogenic opal for ODP 658A/B (% over μg g^{-1} for 658C). (C) Normalized content of $\Sigma C_{30} + C_{32}$ diols (μg g^{-1} over μg g^{-1}). (D) Normalized content of $\Sigma C_{37} + C_{38}$ alkenones (μg g^{-1} over μg g^{-1}). (E) Normalized content of dinosterol (μg g^{-1} over μg g^{-1}). (F) Normalized content of $\Sigma C_{27} + C_{29} + C_{31} + C_{33}$ *n*-alkanes plus $\Sigma C_{24} + C_{26} + C_{28} + C_{30}$ *n*-alkanols (μg g^{-1} over μg g^{-1}).

Thus, nutrient inputs with different ratios of Zn/Co would enhance the productivity of the two groups differently. Future research on the trace metal contents of dust inputs, photic waters and of sediments from the ODP Site 658 area could help test this hypothesis.

5. Conclusions

The estimated productivities of diatoms, dinoflagellates, haptophytes and eustigmatophytes/diatoms (the contents and MARs of opal, dinosterol, alkenones and alkyl diols, respectively) represented the major part of the total phytoplankton paleoproductivity (as expressed by the content of chlorins) at Site 658 over the last 160 kyr. Significant points are:

1. Five high productivity intervals (HPI) are identified, based on the content and MAR of chlorins: two at the glacial/interglacial transition boundaries of 132–122 and 15–8 ka, two within the warmer periods of MIS 3 (50–30 ka) and the late Holocene (4–0 ka), and one within the glacial period of MIS 4 (67–60 ka).
2. Total and individual phytoplankton productivities were the lowest during the penultimate glacial maximum (145–135 ka) and the last glacial maximum (23–18 ka), implying that upwelling was not strong, and/or that the center of the upwelling cell had migrated further offshore (Bertrand et al., 1996). Evidently, the "biological pump" at this location did not contribute significantly to lower atmospheric pCO_2 at those times.
3. Major changes in phytoplankton community structure took place over the last 160 kyr at Site 658 on timescales of hundreds and thousands of years. Community structure changes were characterized by increased diatom contribution to total productivity during the HPI of Terminations I and II, while eustigmatophyte/diatom and haptophyte contributions were higher during MIS 5. Dinosterol made the highest contribution in the Holocene.
4. We observe strong parallels between major portions of the records for the terrigenous biomarker proxy (*n*-alkanes and *n*-alkanols) and those of the total phytoplankton productivity (chlorins). We interpret this parallel behavior as a causal relationship, namely fertilization by nutrients transported within the terrigenous input (Fig. 2).
5. The fertilizing effect of dust inputs is superimposed on that of the nutrients provided by the upwelling of the deep waters, current transport and river input. These fertilizing processes operate positively, but vary independently. Variations in both quantity and composition of the eolian-borne nutrients, related to varying lift off from differing source areas, could explain some of the sequences of changing community structures of the phytoplankton.

Acknowledgments

We thank the NY Sea Grant (M.Z.), Taiwan National Science Council (M.Z. and C.Y.H.), NSF (M.J.H.) and the Natural Environment Research Council (G.E.) for support and the Organic Geochemistry Mass Spectrometry Facility at Bristol for GC-MS access. We thank the ODP for samples, Dr. X. Feng for constructive discussions and Drs. J. Volkman, F. Prahl and L. Méjanell for comments on an earlier draft of this paper. Dr. G. Versteegh and an anonymous reviewer are thanked for helpful and detailed reviews. The data sets will be available from the Pangaea database.

Associate Editor—**J. Grimalt**

References

Abrantes, F., 2000. 200000 yr diatom records from Atlantic upwelling sites reveal maximum productivity during LGM and a shift in phytoplankton community structure at 185000 yr. Earth and Planetary Science Letters 176, 7–16.

Abrantes, F., Meggers, H., Nave, S., Bollman, J., Palma, S., Sprengel, C., Henderiks, J., Spies, A., Salgueiro, E., Moita, T., Neuer, S., 2002. Fluxes of micro-organisms along a productivity gradient in the Canary Islands region (29°N): implications for paleoreconstructions. Deep-Sea Research Part II 49, 3599–3629.

Altabet, M.A., Higginson, M.J., Murray, D.W., 2002. The effect of millennial-scale changes in Arabian Sea denitrification on atmospheric CO_2. Nature 415, 159–162.

Amo, M., Minagawa, M., 2003. Sedimentary record of marine and terrigenous organic matter delivery to the Shatsky Rise, western North Pacific, over the last 130 kyr. Organic Geochemistry 34, 1299–1312.

Anderson, R.F., Chase, Z., Fleisher, M.Q., Sachs, J., 2002. The Southern Ocean's biological pump during the Last Glacial Maximum. Deep-Sea Research Part II 49, 1909–1938.

Armstrong, R.A., Lee, C., Hedges, J.I., Honjo, S., Wakeham, S.G., 2002. A new, mechanistic model for organic carbon fluxes in the ocean based on the quantitative association of POC with ballast minerals. Deep-Sea Research Part II 49, 219–236.

Barcena, M.A., Cacho, I., Abrantes, F., Sierro, F.J., Grimalt, J.O., Flores, J.A., 2001. Paleoproductivity variations related to climatic conditions in the Alboran Sea (western Mediterranean) during the last glacial–interglacial transition: the diatom record. Palaeogeography Palaeoclimatology Palaeoecology 167, 337–357.

Barnola, J.M., Raynaud, D., Korotkevich, Y.S., Lorius, C., 1987. Vostok ice core provides 160,000-year record of atmospheric CO_2. Nature 329, 408–414.

Berger, W.H., Keir, R.S., 1984. Glacial–Holocene changes in atmospheric CO_2 and the deep-sea record. In: Hasen, I.E., Takahashi, T. (Eds.), Climate Processes and Climate Sensitivity. Ameircan Geophysical Union, Washington, pp. 337–351.

Berger, W.H., Smetacek, V.S., Wefer, G., 1989. Ocean productivity and Palaeoproductivity – An Overview. In: Berger, W.H., Smetacek, V.S., Wefer, G. (Eds.), Productivity of the Ocean: Present and Past. John Wiley and Sons Limited, London, pp. 1–34.

Bertrand, P., Shimmield, G., Martinez, P., Grousset, F., Jorissen, F., Paterne, M., Pujol, C., Bouloubassi, I., Buat Menard, P., Peypouquet, J.P., Beaufort, L., Sicre, M.A., Lallier-Verges, E., Foster, J.M., Ternois, Y., 1996. The glacial ocean productivity hypothesis; the importance of regional temporal and spatial studies. Marine Geology 130, 1–9.

Bird, M.I., Summons, R.E., Gagan, M.K., Roksandic, Z., Dowling, L., Head, J., Fifield, L.K., Cresswell, R.G., Johnson, D.P., 1995. Terrestrial vegetation change Inferred from *n*-alkane $\delta^{13}C$ analysis in the marine-environment. Geochimica et Cosmochimica Acta 59, 2853–2857.

Bishop, J.K.B., Davis, R.E., Sherman, J.T., 2002. Robotic observations of dust storm enhancement of carbon biomass in the North Pacific. Science 298, 817–821.

Boon, J.J., Rijpstra, W.I.C., de Lange, F., de Leeuw, J.W., Yoshioka, M., Shimizu, Y., 1979. Black Sea sterol; a molecular fossil for dinoflagellate blooms. Nature 277, 125–127.

Bowie, A.R., Maldonado, M.T., Frew, R.D., Croot, P.L., Achterberg, E.P., Mantoura, R.F.C., Worsfold, P.J., Law, C.S., Boyd, P.W., 2001. The fate of added iron during a mesoscale fertilisation experiment in the Southern Ocean. Deep-Sea Research Part II 48, 2703–2743.

Boyd, P.W., Watson, A.J., Law, C.S., Abraham, E.R., Trull, T., Murdoch, R., Bakker, D.C.E., Bowie, A.R., Buesseler, K.O., Chang, H., Charette, M., Croot, P., Downing, K., Frew, R., Gall, M., Hadfield, M., Hall, J., Harvey, M., Jameson, G., LaRoche, J., Liddicoat, M., Ling, R., Maldonado, M.T., McKay, R.M., Nodder, S., Pickmere, S., Pridmore, R., Rintoul, S., Safi, K., Sutton, P., Strzepek, R., Tanneberger, K., Turner, S., Waite, A., Zeldis, J., 2000. A mesoscale phytoplankton bloom in the polar Southern Ocean stimulated by iron fertilization. Nature 407, 695–702.

Boyd, P.W., Law, C.S., Wong, C.S., Nojiri, Y., Tsuda, A., Levasseur, M., Takeda, S., Rivkin, R., Harrison, P.J., Strzepek, R., Gower, J., McKay, R.M., Abraham, E., Arychuk, M., Barwell-Clarke, J., Crawford, W., Crawford, D., Hale, M., Harada, K., Johnson, K., Kiyosawa, H., Kudo, I., Marchetti, A., Miller, W., Needoba, J., Nishioka, J., Ogawa, H., Page, J., Robert, M., Saito, H., Sastri, A., Sherry, N., Soutar, T., Sutherland, N., Taira, Y., Whitney, F., Wong, S.K.E., Yoshimura, T., 2004. The decline and fate of an iron-induced subarctic phytoplankton bloom. Nature 428, 549–553.

Boyle, E.A., 1988. The role of vertical chemical fractionation in controlling late quaternary atmospheric carbon dioxide. Journal of Geophysical Research-Oceans 93, 15701–15714.

Brassell, S.C., Eglinton, G., Marlowe, I.T., Pflaumann, U., Sarnthein, M., 1986. Molecular stratigraphy; a new tool for climatic assessment. Nature 320, 129–133.

Broecker, W.S., Peng, T.-H., 1982. Tracers in the Sea. Eldigio Press, Palisades, NY.

Broecker, W.S., Peng, T.-H., 1989. The causes of the glacial to interglacial atmospheric CO_2 change: a polar alkalinity hypothesis. Global Biogeochemical Cycles 3, 215–239.

Buesseler, K.O., Andrews, J.E., Pike, S.M., Charette, M.A., 2004. The effects of iron fertilization on carbon sequestration in the Southern Ocean. Science 304, 414–417.

Cacho, I., Grimalt, J.O., Sierro, F.J., Shackleton, N., Canals, M., 2000. Evidence for enhanced Mediterranean thermohaline circulation during rapid climatic coolings. Earth and Planetary Science Letters 183, 417–429.

Calvert, S.E., Pedersen, T.F., 1992. Organic matter accumulation, remineralization and burial in an anoxic coastal sediment. In: Whelan, J.K., Farrington, J.W. (Eds.), Organic Matter: Productivity, Accumulation and Preservation in Recent and Ancient Sediments. Columbia University Press, New York, pp. 231–263.

Calvo, E., Pelejero, C., Logan, G.A., De Deckker, P., 2004. Dust-induced changes in phytoplankton composition in the Tasman Sea during the last four glacial cycles. Paleoceanography 19.

Chrisholm, S.W., Falkowski, P.G., Cullen, J.J., 2001. Discrediting ocean fertilization. Science 294, 309–310.

Coale, K.H., Johnson, K.S., Chavez, P.P., Buesseler, K.O., Barber, R.T., Brzezinski, M.A., Cochlan, W.P., Millero, F.J., Falkowski, P.G., Bauer, J.E., Wanninkhof, R.H., Kudela, R.M., Altabet, M.A., Hales, B.E., Takahashi, T., Landry, M.R., Bidigare, R.R., Wang, X.J., Chase, Z., Strutton, P.G., Friederich, G.E., Gorbunov, M.Y., Lance, V.P., Hilting, A.K., Hiscock, M.R., Demarest, M., Hiscock, W.T., Sullivan, K.F., Tanner, S.J., Gordon, R.M., Hunter, C.N., Elrod, V.A., Fitzwater, S.E., Jones, J.L., Tozzi, S., Koblizek, M., Roberts, A.E., Herndon, J., Brewster, J., Ladizinsky, N., Smith, G., Cooper, D., Timothy, D., Brown, S.L., Selph, K.E., Sheridan, C.C., Twining, B.S., Johnson, Z.I., 2004. Southern ocean iron enrichment experiment: Carbon cycling in high- and low-Si waters. Science 304, 408–414.

Dahl, K.A., Repeta, D.J., Goericke, R., 2004. Reconstructing the phytoplankton community of the Cariaco Basin during the Younger Dryas cold event using chlorin steryl esters. Paleoceanography 19, 19–29.

de Leeuw, J.W., Rijpstra, W.I.C., Schenck, P.A., 1981. The occurrence and identification of C_{30}, C_{31} and C_{32} alkan-1, 15-diols and alkan-15-one-1-ols in Unit-I and Unit-II Black-Sea sediments. Geochimica et Cossmochimica Acta 45, 2281–2285.

deMenocal, P., Ortiz, J., Guilderson, T., Adkins, J., Sarnthein, M., Baker, L., Yarusinsky, M., 2000. Abrupt onset and termination of the African Humid Period: rapid climate responses to gradual insolation forcing. Quaternary Science Reviews 19, 347–361.

Duan, Y., 2000. Organic geochemistry of Recent marine sediments from the Nansha Sea, China. Organic Geochemistry 31, 159–167.

Eckardt, C.B., Pearce, G.E.S., Keely, B.J., Kowalewska, G., Jaffe, R., Maxwell, J.R., 1992. A widespread chlorophyll transformation pathway in the aquatic environment. Organic Geochemistry 19, 217–227.

Eglinton, G., Hamilton, R.J., 1967. Leaf epicuticular waxes. Science 156, 1322–1335.

Eglinton, G., Bradshaw, S.A., Rosell, A., Sarnthein, M., Pflaumann, U., Tiedemann, R., 1992. Molecular record of secular sea-surface temperature changes on 100-year timescales for glacial terminations I, II and IV. Nature 356, 423–426.

Eglinton, T.I., Conte, M.H., Eglinton, G., Hayes, J.M., 2001. In: Proceedings of a workshop on alkenone-based paleoceanographic indicators. Geochemistry Geophysics Geosystems 2, doi:110.1029/2000GC000122.

Eglinton, T.I., Eglinton, G., Dupont, L., Sholkovitz, E.R., Montlucon, D., Reddy, C.M., 2002. Composition, age, and provenance of organic matter in NW African dust over the Atlantic Ocean. Geochemistry Geophysics Geosystems 3. doi:10.1029/2001GC000269.

Eppley, R.W., Peterson, B.J., 1979. Particulate organic matter flux and planktonic new production in the deep ocean. Nature 282, 677–680.

Fernandes, M.B., Sicre, M.A., 2000. The importance of terrestrial organic carbon inputs on Kara Sea shelves as revealed by *n*-alkanes, OC and $\delta^{13}C$ values. Organic Geochemistry 31, 363–374.

Ferreira, A.M., Miranda, A., Caetano, M., Baas, M., Vale, C., Sinninghe Damste, J.S., 2001. Formation of mid-chain alkane keto-ols by post-depositional oxidation of mid-chain diols in Mediterranean sapropels. Organic Geochemistry 32, 271–276.

Furlong, E.T., Carpenter, R., 1988. Pigment preservation and remineralization in oxic coastal marine sediments. Geochimica et Cosmochimica Acta 52, 87–99.

Futterer, D.K., 1983. The modern upwelling record off Northwest Africa. In: Suess, E., Thiede, J. (Eds.), Coastal Upwelling: Its Sedimentary Records. Plenum, New York, pp. 105–121.

Gabric, A.J., Garcia, L., Vancamp, L., Nykjaer, L., Eifler, W., Schrimpf, W., 1993. Offshore export of shelf production in the Cape Blanc (Mauritania) giant filament as derived from Coastal Zone Color Scanner Imagery. Journal of Geophysical Research-Oceans 98, 4697–4712.

Gagosian, R.B., Peltzer, E.T., Zafiriou, O.C., 1981. Atmospheric transport of continentally derived lipids to the tropical North Pacific. Nature 291, 312–315.

Goudie, A.S., Middleton, N.J., 2001. Saharan dust storms; nature and consequences. Earth-Science Reviews 56, 179–204.

Grousset, F.E., Parra, M., Bory, A., Martinez, P., Bertrand, P., Shimmield, G., Ellam, R.M., 1998. Saharan wind regimes traced by the Sr-Nd isotopic composition of subtropical Atlantic sediments: Last Glacial maximum vs today. Quaternary Science Reviews 17, 395–409.

Harris, P.G., Maxwell, J.R., 1995. A novel method for the rapid determination of chlorin concentrations at high stratigraphic resolution in marine sediments. Organic Geochemistry 23, 853–856.

Harris, P.G., Zhao, M., Rosell-Mele, A., Tiedemann, R., Sarnthein, M., Maxwell, J.R., 1996. Chlorin accumulation rate as a proxy for Quaternary marine primary productivity. Nature 383, 63–65.

Hartnett, H.E., Keil, R.G., Hedges, J.I., Devol, A.H., 1998. Influence of oxygen exposure time on organic carbon preservation in continental margin sediments. Nature 391, 572–574.

Hartnett, H.E., Devol, A.H., 2003. Role of a strong oxygen-deficient zone in the preservation and degradation of organic matter: a carbon budget for the continental margins of northwest Mexico and Washington State. Geochimica et Cosmochimica Acta 67, 247–264.

Hedges, J.I., Keil, R.G., 1995. Sedimentary organic matter preservation: an assessment and speculative synthesis. Marine Chemistry 49, 81–115.

Henriksson, A.S., Sarnthein, M., Eglinton, G., Poynter, J., 2000. Dimethylsulfide production variations over the past 200 k.y. in the equatorial Atlantic: a first estimate. Geology 28, 499–502.

Higginson, M.J., 2000. Chlorin pigment stratigraphy as a new and rapid paleoceanographic proxy in the Quaternary. Ph.D. thesis, University of Bristol, Bristol.

Higginson, M.J., Maxwell, J.R., Altabet, M.A., 2003. Nitrogen isotope and chlorin paleoproductivity records from the Northern South China Sea: remote vs. local forcing of millennial- and orbital-scale variability. Marine Geology 201, 223–250.

Higginson, M.J., Altabet, M.A., 2004. Initial test of the silicic acid leakage hypothesis using sedimentary biomarkers. Geophysical Research Letters 31, L18303. doi:10.1029/2004GL020511.

Higginson, M.J., Altabet, M.A., Murray, D.W., Murray, R.W., Herbert, T.D., 2004. Geochemical evidence for abrupt changes in relative strength of the Arabian monsoons during a stadial/interstadial climate transition. Geochimica et Cosmochimica Acta 68, 3807–3826.

Hinrichs, K.U., Schneider, R.R., Mueller, P.J., Rullkoetter, J., 1999. A biomarker perspective on paleoproductivity variations in two late Quaternary sediment sections from the Southeast Atlantic Ocean. Organic Geochemistry 30, 341–366.

Hoefs, M.J.L., Rijpstra, W.I.C., Sinninghe Damsté, J.S., 2002. The influence of oxic degradation on the sedimentary biomarker record I: evidence from Madeira Abyssal Plain turbidites. Geochimica et Cosmochimica Acta 66, 2719–2735.

Hooghiemstra, H., 1989. Variations of the NW African trade wind regime during the last 140,000 years; changes in pollen flux evidenced by marine sediment records. In: Leinen, M., Sarnthein, M. (Eds.), Paleoclimatology and Paleometeorology; Modern and Past Patterns of Global Atmospheric Transport. D. Reidel Publishing Company, Dordrecht–Boston, pp. 733–770.

Huang, Y.S., Dupont, L., Sarnthein, M., Hayes, J.M., Eglinton, G., 2000. Mapping of C-4 plant input from North West Africa into North East Atlantic sediments. Geochimica et Cosmochimica Acta 64, 3505–3513.

Huntsman, S.A., Barber, R.T., 1977. Primary production off Northwest Africa: relationship to wind and nutrient conditions. Deep-Sea Research 24, 25–33.

Ikehara, M., Kawamura, K., Ohkouchi, N., Murayama, M., Nakamura, T., Taira, A., 2000. Variations of terrestrial input and marine productivity in the Southern Ocean (48°S) during the last two deglaciations. Paleoceanography 15, 170–180.

Ishiwatari, R., Hirakawa, Y., Uzaki, M., Yamada, K., Yada, T., 1994. Organic geochemistry of the Japan Sea sediments; 1. Bulk organic matter and hydrocarbon analyses of core KH-79-3, C-3 from the Oki Ridge for paleoenvironment assessments. Journal of Oceanography 50, 179–195.

Ishiwatari, R., Yamada, K., Matsumoto, K., Houtatsu, M., Naraoka, H., 1999. Organic molecular and carbon isotopic records of the Japan Sea over the past 30 kyr. Paleoceanography 14, 260–270.

Ittekkot, V., Haake, B., 1990. The terrestrial link in the removal of organic carbon in the sea. In: Ittekkot, V., Kempe, S., Michaelis, W., Spitzy, A. (Eds.), Facets of Modern Biogeochemistry. Springer-Verlag, Berlin, pp. 318–324.

Jasper, J.P., Hayes, J.M., 1990. A carbon isotope record of CO_2 levels during the Late Quaternary. Nature 347, 462–464.

Jordan, R.W., Zhao, M., Eglinton, G., Weaver, P.P.E., 1996. Coccolith and alkenone stratigraphy and palaeoceanography at an upwelling site off NW Africa (ODP 658C) during the last 130, 000 years. In: Moguilevsky, A., Whatley, R. (Eds.), Microfossils and Oceanic Environments. University of Wales, Aberystwyth-Press, pp. 111–130.

Keely, B.J., Prowse, W.G., Maxwell, J.R., 1990. The Treibs hypothesis: an evaluation based on structural studies. Energy & Fuels 4, 628–634.

Kennedy, J.A., Brassell, S.C., 1992. Molecular stratigraphy of the Santa Barbara Basin; comparison with historical records of annual climate change. Organic Geochemistry 19, 235–244.

Leroux, M., 1993. The mobile polar-high – a new concept explaining present mechanisms of meridional air-mass and energy exchanges and global propagation of paleoclimatic changes. Global and Planetary Change 7, 69–93.

Longhurst, A., Sathyendranath, S., Platt, T., Caverhill, C., 1995. An estimate of global primary production in the ocean from satellite radiometer data. Journal of Plankton Research 17, 1245–1271.

Mackey, D.J., Blanchot, J., Higgins, H.W., Neveux, J., 2002. Phytoplankton abundances and community structure in the equatorial Pacific. Deep-Sea Research Part II 49, 2561–2582.

Mackey, M.D., Mackey, D.J., Higgins, H.W., Wright, S.W., 1996. CHEMTAX – A program for estimating class abundances from chemical markers: application to HPLC measurements of phytoplankton. Marine Ecology-Progress Series 144, 265–283.

Madureira, L.A.S., van Kreveld, S.A., Eglinton, G., Conte, M.H., Ganssen, G., van Hinte, J.E., Ottens, J.J., 1997. Late Quaternary high-resolution biomarker and other sedimentary climate proxies in a Northeast Atlantic core. Paleoceanography 12, 255–269.

Mangelsdorf, K., Guntner, U., Rullkotter, J., 2000. Climatic and oceanographic variations on the California continental margin during the last 160 kyr. Organic Geochemistry 31, 829–846.

Marlowe, I.T., Brassell, S.C., Eglinton, G., Green, J.C., 1990. Long-chain alkenones and alkyl alkenoates and the fossil coccolith record of marine sediments. Chemical Geology 88, 349–375.

Martin, J.H., Fitzwater, S.E., 1988. Iron-deficiency limits phytoplankton growth in the northeast Pacific subarctic. Nature 331, 341–343.

Martinez, P., Bertrand, P., Shimmield, G.B., Cochrane, K., Jorissen, F.J., Foster, J., Dignan, M., 1999. Upwelling intensity and ocean productivity changes off Cape Blanc (northwest Africa) during the last 70,000 years: geochemical and micropalaeontological evidence. Marine Geology 158, 57–74.

McCave, I.N., 2002. A poisoned chalice? Science 298, 1186–1187.

Méjanelle, L., Sanchez-Gargallo, A., Bentaleb, I., Grimalt, J.O., 2003. Long chain *n*-alkyl diols, hydroxy ketones and sterols in a marine eustigmatophyte, *Nannochloropsis gaditana*, and in *Brachionus plicatilis* feeding on the algae. Organic Geochemistry 34, 527–538.

Menzel, D., van Bergen, P.P., Schouten, S., Sinninghe Damste, J.S., 2003. Reconstruction of changes in export productivity during Pliocene sapropel deposition; a biomarker approach. Palaeogeography, Palaeoclimatology, Palaeoecology 190, 273–287.

Mills, M.M., Ridame, C., Davey, M., La Roche, J., Geider, R.J., 2004. Iron and phosphorus co-limit nitrogen fixation in the eastern tropical North Atlantic. Nature 429, 292–294.

Mix, A.C., 1989. Influence of productivity variations on long-term atmospheric CO_2. Nature 337, 541–544.

Moldowan, J.M., Dahl, J., Jacobson, S.R., Huizinga, B.J., Fago, F.J., Shetty, R., Watt, D.S., Peters, K.E., 1996. Chemostratigraphic reconstruction of biofacies: molecular evidence linking cyst-forming dinoflagellates with pre-Triassic ancestors. Geology 24, 159–162.

Morel, F.M.M., Reinfelder, J.R., Roberts, S.B., Chamberlain, C.P., Lee, J.G., Yee, D., 1994. Zinc and carbon co-limitation of marine phytoplankton. Nature 369, 740–742.

Moreno, A., Nave, S., Kuhlmann, H., Canals, M., Targarona, J., Freudenthal, T., Abrantes, F., 2002. Productivity response in the North Canary Basin to climate changes during the last 250,000 yr; a multi-proxy approach. Earth and Planetary Science Letters 196, 147–159.

Moreno, A., Cacho, I., Canals, M., Grimalt, J.O., Sanchez-Vidal, A., 2004. Millennial-scale variability in the productivity signal from the Alboran Sea record, Western Mediterranean Sea. Palaeogeography Palaeoclimatology Palaeoecology 211, 205–219.

Mueller, P.J., Suess, E., 1979. Productivity, sedimentation rate, and sedimentary organic matter in the oceans; I. Organic carbon preservation. Deep-Sea Research Part A 26, 1347–1362.

Oldenburg, T.B.P., Rullkoetter, J., Boettcher, M.E., Nissenbaum, A., 2000. Molecular and isotopic characterization of organic matter in recent and sub-recent sediments from the Dead Sea. Organic Geochemistry 31, 251–265.

Pailler, D., Bard, E., Rostek, F., Zheng, Y., Mortlock, R., van Geen, A., 2002. Burial of redox-sensitive metals and organic matter in the equatorial Indian Ocean linked to precession. Geochimica et Cosmochimica Acta 66, 849–865.

Paytan, A., Kastner, M., Chavez, P.P., 1996. Glacial to interglacial fluctuations in productivity in the Equatorial Pacific as indicated by marine barite. Science 274, 1355–1357.

Pedersen, T.F., Calvert, S.E., 1990. Anoxia vs productivity; what controls the formation of organic-carbon-rich sediments and sedimentary rocks. AAPG Bulletin 74, 454–466.

Pelejero, C., Kienast, M., Wang, L.J., Grimalt, J.O., 1999. The flooding of Sundaland during the last deglaciation: imprints in hemipelagic sediments from the southern South China Sea. Earth and Planetary Science Letters 171, 661–671.

Pelejero, C., 2003. Terrigenous *n*-alkane input in the South China Sea: high-resolution records and surface sediments. Chemical Geology 200, 89–103.

Perez-Marrero, J., Llinas, O., Maroto, L., Rueda, M.J., Cianca, A., 2002. Saharan dust storms over the Canary Islands during winter 1998 as depicted from the advanced very high-resolution radiometer. Deep-Sea Research Part II 49, 3465–3479.

Petit, J.R., Jouzel, J., Raynaud, D., Barkov, N.I., Barnola, J.M., Basile, I., Bender, M., Chappellaz, J., Davis, M., Delaygue, G., Delmotte, M., Kotlyakov, V.M., Legrand, M., Lipenkov, V.Y., Lorius, C., Pepin, L., Ritz, C., Saltzman, E., Stievenard, M., 1999. Climate and atmospheric history of the past 420,000 years from the Vostok ice core, Antarctica. Nature 399, 429–436.

Pokras, E.M., 1987. Diatom record of late Quaternary climatic changes in the eastern equatorial Atlantic and tropical Africa. Paleoceanography 2, 273–286.

Poynter, J., 1989. The recongnition of paleoclimatic signals in organic geochemical data. Ph.D. thesis, University of Bristol, Bristol.

Poynter, J., Farrimond, P., Brassell, S.C., Eglinton, G., 1989a. Molecular stratigraphic study of sediments from Holes 658A and 660A, Leg 108. Proceedings of the Ocean Drilling Program, Scientific Results 108, 387–394.

Poynter, J., Eglinton, G., 1991. The biomarker concept: strengths and weaknesses. Fresenius Journal of Analytical Chemistry 339, 725–731.

Poynter, J.G., Farrimond, P., Robinson, N., Eglinton, G., 1989b. Aeolian-derived higher plant lipids in the marine sedimentary record; links with palaeoclimate. In: Leinen, M., Sarnthein, M. (Eds.), Paleoclimatology and Paleometeorology: Modern and Past patterns of Global Atmospheric Tansport. D. Reidel Publishing Company, Dordrecht–Boston, pp. 435–462.

Prahl, F.G., Wakeham, S.G., 1987. Calibration of unsaturation patterns in long-chain ketone compositions for paleotemperature assessment. Nature 330, 367–369.

Prahl, F.G., Muehlhausen, L.A., Lyle, M., 1989. An organic geochemical assessment of oceanographic conditions at the MANOP site C over the past 26,000 years. Paleoceanography 4, 495–510.

Prahl, F.G., Collier, R.B., Dymond, J., Lyle, M., Sparrow, M.A., 1993. A biomarker perspective on prymnesiophyte productivity in the northeast Pacific Ocean. Deep-Sea Research Part I 40, 2061–2076.

Price, N.M., Morel, F.M.M., 1990. Cadmium and cobalt substitution for zinc in a marine diatom. Nature 344, 658–660.

Prospero, J.M., Ginoux, P., Torres, O., Nicholson, S.E., Gill, T.E., 2002. Environmental characterization of global sources of atmospheric soil dust identified with the Nimbus 7 Total Ozone Mapping Spectrometer (TOMS) absorbing aerosol product. Reviews of Geophysics 40, 1002. doi:10.1029/2000RG000095.

Qian, Y.R., Jochens, A.E., Kennicutt, M.C., Biggs, D.C., 2003. Spatial and temporal variability of phytoplankton biomass and community structure over the continental margin of the northeast Gulf of Mexico based on pigment analysis. Continental Shelf Research 23, 1–17.

Ragueneau, O., Treguer, P., Leynaert, A., Anderson, R.F., Brzezinski, M.A., DeMaster, D.J., Dugdale, R.C., Dymond, J., Fischer, G., Francois, R., Heinze, C., Maier-Reimer, E., Martin-Jezequel, V., Nelson, D.M., Queguiner, B., 2000. A review of the Si cycle in the modem ocean: recent progress and missing gaps in the application of biogenic opal as a paleoproductivity proxy. Global and Planetary Change 26, 317–365.

Repeta, D.J., McCaffrey, M.A., Farrington, J.W., 1992. Organic geochemistry as a tool to study upwelling systems; recent results from the Peru and Namibian shelves. In: Summerhayes, C.P., Prell, W.L., Emeis, K.C. (Eds.), Upwelling Systems: Evolution since the Early Miocene. Geological Society, London, pp. 257–272.

Romankevich, E.A., 1984. Geochemistry of Organic Matter in the Ocean. Springer-Verlag, New York.

Rostek, F., Bard, E., Beaufort, L., Sonzoni, C., Ganssen, G., 1997. Sea surface temperature and productivity records for the past 240 kyr in the Arabian Sea. Deep-Sea Research II 44, 1461–1480.

Ruddiman, W.F., 1997. Tropical Atlantic terrigenous fluxes since 25, 000 yrs BP. Marine Geology 136, 189–207.

Sarnthein, M., Thiede, J., Pflaumann, U., Erlenkeuser, H., Fuetterer, D.K., Koopmann, B., Lange, H., Seibold, E., 1982. Atmospheric and oceanic circulation patterns off Northwest Africa during the past 25 million years. In: Von Rad, U., Hinz, K., Sarnthein, M., Seibold, E. (Eds.), Geology of the Northwest African continental margin. Springer-Verlag, Berlin, pp. 545–604.

Sarnthein, M., Pflaumann, U., Ross, R., Tiedemann, R., Winn, K., 1992. Transfer functions to reconstruct ocean paleoproductivity: a comparison. In: Summerhayes, C.P., Prell, W.L., Emeis, K.C. (Eds.), Upwelling Systems: Evolution since the early Miocene. Geological Society, London.

Schouten, S., Hoefs, M.J.L., Sinninghe Damste, J.S., 2000. A molecular and stable carbon isotopic study of lipids in late Quaternary sediments from the Arabian Sea. Organic Geochemistry 31, 509–521.

Schubert, C.J., Villanueva, J., Calvert, S.E., Cowie, G.L., von Rad, U., Schultz, H., Berner, U., Erlenkeuser, H., 1998. Stable phytoplankton community structure in the Arabian Sea over the past 200,000 years. Nature 394, 563–566.

Schulte, S., Bard, E., 2003. Past changes in biologically mediated dissolution of calcite above the chemical lysocline recorded in Indian Ocean sediments. Quaternary Science Reviews 22, 1757–1770.

Seki, O., Kawamura, k., Nakatsuka, T., Ohnishi, K., Ikehara, M., Wakatsuchi, M., 2003. Sediment core profiles of long-chain *n*-alkanes in the Sea of Okhotsk: enhanced transport of terrestrial organic matter from the last deglaciation to the early Holocene. Geophysical Research Letters 30.

Seki, O., Ikehara, M., Kawamura, K., Nakatsuka, T., Ohnishi, K., Wakatsuchi, M., Narita, H., Sakamoto, T., 2004. Reconstruction of paleoproductivity in the Sea of Okhotsk over the last 30 kyr. Paleoceanography 19.

Shackleton, N.J., Hall, M.A., Line, J., Shuxi, C., 1983. Carbon isotope data in Core V19-30 confirm reduced carbon dioxide concentration in the ice-age atmosphere. Nature 306, 319–322.

Shankle, A.M., Goericke, R., Franks, P.J.S., Levin, L.A., 2002. Chlorin distribution and degradation in sediments within and below the Arabian Sea oxygen minimum zone. Deep-Sea Research Part 149, 953–969.

Shimmield, G.B., 1992. Can sediment geochemistry record changes in coastal upwelling palaeoproductivity? Evidence from north-west Africa and the Arabian Sea. In: Summerhayes, C.P., Prell, W.L., Emeis, K.C. (Eds.), Upwelling Systems: Evolution Since the Early Miocene. Geological Society, London, pp. 29–46.

Sicre, M.A., Ternois, Y., Paterne, M., Boireau, A., Beaufort, L., Martinez, P., Bertrand, P., 2000. Biomarker stratigraphic records over the last 150 kyears off the NW African coast at 25°N. Organic Geochemistry 31, 577–588.

Sicre, M.A., Ternois, Y., Paterne, M., Martinez, P., Bertrand, P., 2001. Climatic changes in the upwelling region off Cap Blanc, NW Africa, over the last 70 kyear: a multi- biomarker approach. Organic Geochemistry 32, 981–990.

Simoneit, B.R.T., Chester, R., Eglinton, G., 1977. Biogenic lipids in particulates from lower atmosphere over eastern Atlantic. Nature 267, 682–685.

Sinninghe Damsté, J.S., Rijpstra, W.I.C., Reichart, G.J., 2002. The influence of oxic degradation on the sedimentary biomarker record II. Evidence from Arabian Sea sediments. Geochimica et Cosmochimica Acta 66, 2737–2754.

Sinninghe Damsté, J.S., Rampen, S., Irene, W., Rijpstra, C., Abbas, B., Muyzer, G., Schouten, S., 2003. A diatomaceous origin for long-chain diols and mid-chain hydroxy methyl alkanoates widely occurring in Quaternary marine sediments; indicators for high-nutrient conditions. Geochimica et Cosmochimica Acta 67, 1339–1348.

Smayda, T.J., Reynolds, C.S., 2001. Community assembly in marine phytoplankton: application of recent models to harmful dinoflagellate blooms. Journal of Plankton Research 23, 447–461.

Stein, R., ten Haven, H.L., Littke, R., Rullkoetter, J., Welte, D.H., 1989. Accumulation of marine and terrigenous organic carbon at upwelling Site 658 and nonupwelling sites 657 and 659; implications for the reconstruction of paleoenvironments in the eastern subtropical Atlantic through late Cenozoic times. Proceedings of the Ocean Drilling Program, Scientific Results 108, 361–385.

Suess, E., 1980. Particulate organic carbon flux in the oceans: surface productivity and oxygen utilization. Nature 288, 260–263.

Summerhayes, C.P., Kroon, D., Rosell-Mele, A., Jordan, R.W., Schrader, H.J., Hearn, R., Villanueva, J., Grimalt, J.O., Eglinton, G., 1995. Variability in the Benguela current upwelling system over the past 70,000 years. Progress in Oceanography 35, 207–251.

Sunda, W.G., Huntsman, S.A., 1995. Cobalt and zinc interreplacement in marine phytoplankton: biological and geochemical implications. Limnology and Oceanography 40, 1404–1417.

ten Haven, H.L., Rullkoetter, J., Stein, R., 1989. Preliminary analysis of extractable lipids in sediments from the eastern North Atlantic (Leg 108); comparison of a coastal upwelling area (Site 658) with a nonupwelling area (Site 659). Proceedings of the Ocean Drilling Program, Scientific Results 108, 351–360.

Ternois, Y., Kawamura, K., Keigwin, L., Ohkouchi, N., Nakatsuka, T., 2001. A biomarker approach for assessing marine and terrigenous inputs to the sediments of Sea of Okhotsk for the last 27,000 years. Geochimica et Cosmochimica Acta 65, 791–802.

Thomson, J., Nixon, S., Summerhayes, C.P., Rohling, E.J., Schoenfeld, J., Zahn, R., Grootes, P., Abrantes, R., Caspar, L., Vaqueiro, S., Rothwell, R.G., 2000. Enhanced productivity on the Iberian margin during glacial interglacial transitions revealed by barium and diatoms. Journal of the Geological Society of London 157, 667–677.

Tiedemann, R., Sarnthein, M., Stein, R., 1989. Climatic changes in the Western Sahara: Aeolo-marine sediment record of the last 8 million years (Sites 657–661). Proceedings of the Ocean Drilling Program, Scientific Results 108, 241–278.

Tiedemann, R., 1991. Acht Millionen Jahre Klimageschichte von Nordwest Afrika und Palozeanographie des angrenzenden Atlantiks: Hochauflosende Zeitreihen von ODP Sites 658–661. Ph.D. thesis, University of Kiel, Kiel, Germany.

Tyson, R.V., 2001. Sedimentation rate, dilution, preservation and total organic carbon; some results of a modelling study. Organic Geochemistry 32, 333–339.

Versteegh, G.J.M., Bosch, H.J., de Leeuw, J.W., 1997. Potential palaeoenvironmental information of C_{24} to C_{36} mid-chain diols, keto-ols and mid-chain hydroxy fatty acids; a critical review. Organic Geochemistry 27, 1–13.

Versteegh, G.J.M., Jansen, J.H.F., De Leeuw, J.W., Schneider, R.R., 2000. Mid-chain diols and keto-ols in SE Atlantic sediments; a new tool for tracing past sea surface water masses? Geochimica et Cosmochimica Acta 64, 1879–1892.

Versteegh, G.J.M., Zonneveld, K.A.F., 2002. Use of selective degradation to separate preservation from productivity. Geology 30, 615–618.

Villanueva, J., Grimalt, J.O., Cortijo, E., Vidal, L., Labeyrie, L., 1997. A biomarker approach to the organic matter deposited in the North Atlantic during the last climatic cycle. Geochimica et Cosmochimica Acta 61, 4633–4646.

Villanueva, J., Grimalt, J.O., Labeyrie, L.D., Cortijo, E., Vidal, L., Louis-Turon, J., 1998. Precessional forcing of productivity in the North Atlantic Ocean. Paleoceanography 13, 561–571.

Volkman, J.K., Eglinton, G., Corner, E.D.S., Forsberg, T.E.V., 1980a. Long-chain alkenes and alkenones in the marine coccolithophorid *Emiliania huxleyi*. Phytochemistry 19, 2619–2622.

Volkman, J.K., Eglinton, G., Corner, E.D.S., Sargent, J.R., 1980b. Novel unsaturated straight-chain C_{37}–C_{39} methyl and ethyl ketones in marine sediments and coccolithophore *Emiliania huxleyi*. In: Douglas, A.G., Maxwell, J.R. (Eds.), Advances in Organic Geochemistry. Pergamon, Oxford, pp. 219–227.

Volkman, J.K., Barrett, S.M., Blackburn, S.I., Mansour, M.P., Sikes, E.L., Gelin, F., 1998. Microalgal biomarkers; a review of recent research developments. Organic Geochemistry 29, 1163–1179.

Volkman, J.K., Barrett, S.M., Blackburn, S.I., 1999. Eustigmatophyte microalgae are potential sources of C_{29} sterols, C_{22}–C_{28} *n*-alcohols and C_{28}–C_{32} *n*-alkyl diols in freshwater environments. Organic Geochemistry 30, 307–318.

Wakeham, S.G., Peterson, M.L., Hedges, J.I., Lee, C., 2002. Lipid biomarker fluxes in the Arabian Sea, with a comparison to the equatorial Pacific Ocean. Deep-Sea Research Part II 49, 2265–2301.

Wells, M.L., 2003. The level of iron enrichment required to initiate diatom blooms in HNLC waters. Marine Chemistry 82, 101–114.

Welschmeyer, N.A., Lorenzen, C.J., 1985. Chlorophyll budgets: zooplankton grazing and phytoplankton growth in a temperate fjord and the Central Pacific gyres. Limnology and Oceanography 30, 1–21.

Werne, J.P., Hollander, D.J., Lyons, T.W., Peterson, L.C., 2000. Climate-induced variations in productivity and planktonic ecosystem structure from the Younger Dryas to Holocene in the Cariaco Basin, Venezuela. Paleoceanography 15, 19–29.

White, F., 1983. The Vegetation of Africa. UNESCO, Paris.

Zhao, M., Beveridge, N.A.S., Shackleton, N.J., Sarnthein, M., Eglinton, G., 1995. Molecular stratigraphy of cores off Northwest Africa: sea surface temperature history over the last 80 ka. Paleoceanography 10, 661–675.

Zhao, M., Eglinton, G., Haslett, S.K., Jordan, R.W., Sarnthein, M., Zhang, Z., 2000. Marine and terrestrial biomarker records for the last 35,000 years at ODP Site 658C off NW Africa. Organic Geochemistry 31, 919–930.

Zhao, M., Dupont, L., Eglinton, G., Teece, M., 2003. *n*-alkane and pollen reconstruction of terrestrial climate and vegetation for N.W. Africa over the last 160 kyr. Organic Geochemistry 34, 131–143.

Zimmerman, A.R., Canuel, E.A., 2002. Sediment geochemical records of eutrophication in the mesohaline Chesapeake Bay. Limnology and Oceanography 47, 1084–1093.